THE ASTROPHYSICAL JOURNAL, 287:586–609, 1984 December 15


# OLD STELLAR POPULATIONS. I. A SPECTROSCOPIC COMPARISON OF GALACTIC GLOBULAR CLUSTERS, M31 GLOBULAR CLUSTERS, AND ELLIPTICAL GALAXIES[1]

DAVID BURSTEIN
Physics Department, Arizona State University, Tempe

S. M. FABER
Lick Observatory; and Board of Studies in Astronomy and Astrophysics, University of California, Santa Cruz

C. M. GASKELL
Lick Observatory; and Board of Studies in Astronomy and Astrophysics, University of California, Santa Cruz, and Department of Astronomy, University of Texas, Austin

AND

N. KRUMM
Lick Observatory; and Board of Studies in Astronomy and Astrophysics, University of California, Santa Cruz, and Department of Astronomy, University of Cincinnati

*Received 1984 January 11; accepted 1984 June 25*

## ABSTRACT

Integrated spectra at 9 Å resolution in the region 4000–6300 Å are presented for 17 Galactic globular clusters and 19 M31 globular clusters. Indices for 11 molecular bands and lines are measured: the CN 4215 Å band, the G band, H$\beta$, Mg *b* and MgH, two Fe I blends, Na D, and two TiO bands. The index $Mg_2$ (measuring Mg *b* and MgH) appears to be a good relative metallicity indicator for Galactic globular clusters, comparable to Zinn's $Q_{39}$ index.

These indices and several broad-band colors are compared between the M31 and Galactic cluster systems, and also with the nuclei of 170 E galaxies. Most of the line indices show smooth sequences with no offsets or discontinuities when the three populations are compared. However, H$\beta$ and CN differ markedly among the three groups. CN is enhanced significantly in several M31 globulars with respect to both Milky Way globulars and the nuclei of E galaxies. Metal-rich and intermediate M31 globulars also have significantly stronger Balmer lines than Galactic globulars, but *not* when compared with E galaxy nuclei. For selected objects, differences also show up in the far-ultraviolet colors. These differences are in conflict with the usual assumption that globular clusters and E galaxies constitute a homogeneous family of old stellar populations, with mean metallicity as the only major variable. Apparently the three old stellar populations examined here must differ in one or more respects beyond mean metallicity.

Several models are analyzed to account for the higher H$\beta$ and CN in M31 globulars, including anomalously hot horizontal branches, blue stragglers, and younger age. Most models fail to give the required simultaneous H$\beta$ and CN enhancements, except possibly those with younger age. Perhaps the present cluster sample in M31 is contaminated by several relatively young disk clusters. Models for M32 seem to require many late F stars as opposed to hotter types, a requirement that also favors younger age. However, there are difficulties with any picture in which M31 clusters and M32 are all assumed to be young, including the fact that CN is very different in the two populations. Because of this, no fully consistent interpretation of all three population groups is as yet apparent. Satellite ultraviolet flux measurements will eventually offer an important means of discriminating between various possible warm-star components.

*Subject headings:* clusters: globular — galaxies: individual — galaxies: nuclei — galaxies: stellar content — stars: abundances

## I. INTRODUCTION

Since Baade (1944) first discovered differences among the stellar populations of M31, the study of stellar populations has been one of increasing diversity and complexity (cf. reviews by King 1971 and Faber 1977). We now know, for example, that not all old stars are metal-poor, nor are all young stars metal-rich. The stellar evolution of stars in globular clusters in our own Galaxy is affected by at least one parameter in addition to metal abundance (Kraft 1979). The existence of young globular clusters in the Magellanic Clouds (Searle, Wilkinson, and Bagnuolo 1980) demonstrates that not all globular clusters everywhere are old.

In the midst of these new developments, one assumption has remained relatively constant, namely, that the globular clusters in our own Galaxy and in M31 are as old as the stars in elliptical galaxies, differing from them only in metal abundance (Baum 1955; Faber 1973*a*; O'Connell 1976). These old stellar populations are commonly thought of as constituting a homogeneous, one-parameter family, with metallicity as the principal variable (Faber 1973*a*; Frogel, Persson, and Cohen 1980; Aaronson *et al.* 1978; Burstein 1979). If such a picture is valid, all objects in this family should populate a one-dimensional continuum with no visible discontinuities when plotted in a multidimensional space of color and spectral-line strength.

This paper reexamines this hypothesis using new and more accurate spectral-line measurements of E galaxies and globular

[1] *Lick Observatory Bulletin*, No. 986.

clusters. Surprisingly, although these populations do appear to form unbroken continua in most indices, significant differences show up in Hβ, CN, and the far-ultraviolet colors. The net conclusion is that the three groups apparently differ from one another in one or more important parameters besides mean metal abundance. These differences somehow involve the warm-star populations in these objects. In addition, there may also be some internal inhomogeneity within groups, most notably among the M31 globulars. Some preliminary ideas are offered to explain these effects, but unfortunately none are as yet completely satisfactory. Ultraviolet satellite flux data, which are a sensitive discriminator for various types of warm-star populations, would be a great aid in forming a more complete picture.

In addition to the M31 and Galactic globulars, the discussion also utilizes an extensive library of stars in the solar neighborhood and in nearby globular clusters. The K giant data in this library will be published soon (Faber *et al.* 1984*a*). Comparison is also made to a large sample of normal elliptical-galaxy nuclei of moderate- to high-line strengths (Faber *et al.* 1984*b*). The cluster observations were previously discussed in a preliminary way by Burstein *et al.* (1981), but the M31 sample has been increased substantially since then, leading now to somewhat different conclusions.

Since the paper is rather lengthy, we suggest that the reader not interested in details quickly scan the observational results in Figures 5*a*–5*l* and then skip directly to § III*g*, where a brief summary of the observations is given. The main discussion then continues in § IV.

## II. OBSERVATIONS

All observations of clusters, stars, and galaxies have been made with the image dissector scanner (IDS; Robinson and Wampler 1972) at the Cassegrain focus of the 3 m Shane Telescope of the Lick Observatory. A full description of the observing procedures is given by Faber *et al.* (1984*a*). Briefly, all program objects were observed with a 600 line grating blazed at 5000 Å, yielding approximately 2300 Å of spectrum from 4000 Å to 6300 Å over 2048 data channels. The spectrograph was used in a dual-slit mode, with slits separated by 35″. The standard observing procedure for point sources alternated star and sky in each aperture. This procedure was modified for Galactic clusters, as described below.

The raw spectra were normalized and reduced to a linear wavelength scale of 1.25 Å per channel. The spectra were not placed on an absolute flux scale but were instead normalized by a quartz-lamp spectrum, exposed always in the same manner. The data for the Galactic clusters were taken during three observing sessions from 1977 June to 1981 August and for the M31 clusters during four sessions from 1977 October to 1981 August. The data for the stars and galaxies were taken from 1972 to 1982. Nightly calibrations based on spectra of nine K giant standard stars ensured that all absorption lines and molecular bands are on a homogeneous system (Faber *et al.* 1984*a*).

All but one of the M31 clusters were observed with a 1.″4 × 4″ slit, giving a spectral resolution of 9 Å (FWHM). (V29 was observed with a 4″ × 4″ slit, giving ~12 Å resolution.) For Galactic clusters, it was necessary to synthesize a larger aperture size to sample most of the cluster light. This was done by computer-controlled raster scanning of the telescope to synthesize a square aperture 66″ × 66″, with one slit centered on the cluster. Since the separation of the slits was smaller than the synthesized aperture, sky scans were obtained by moving off the cluster (these were also raster-scanned). For a number of the larger Galactic clusters, the off-center slit also contained significant information and was flux-averaged with the centered-slit data. In addition, the sky background for many of the metal-rich clusters in both the Galaxy and M31 was contaminated by background starlight. In all cases of serious contamination (at most 10% of the object flux), "sky" was taken to be an average of separate observations of four positions, north, east, west, and south of the cluster.

The spectra are presented in Figures 1*a*–1*d*, in ascending order of absorption-line strength. Insofar as possible, they are paired by metallicity between the Galaxy and M31. The average metric size of the measuring apertures on the Galactic globular clusters is about a factor of 2 smaller than for the M31 clusters. However, the measuring apertures for all clusters are well over one core radius in extent (Harris and Racine 1979).

## III. THE GLOBULAR CLUSTER DATA

### *a) Line Indices and Other Data*

Ten absorption-line indices were measured for each spectrum, including the G band at 4303 Å, the CN feature with bandhead at 4215 Å, the Mg *b* + MgH feature, Mg *b* alone, MgH alone, Hβ, the Fe-dominated blends at 5270 and 5335 Å, the Na D doublet (unresolved), and the TiO band at 5940 Å. A second TiO band at 6190 Å was measured for all the M31 clusters and for several Galactic clusters.

Each line index is a measurement of the flux contained in a wavelength region centered on the feature relative to that contained in red and blue "continuum" regions close to the feature (for details see Faber *et al.* 1984*a*). The widths of central and continuum regions were chosen to minimize the effect of typical galaxy velocity dispersions on the measured absorption-line strengths. The interval specifications for each line index are given in Table 1. The equivalent widths of

TABLE 1

WAVELENGTH INTERVALS FOR INDICES

| Identification | Features Measured | Central Bandpass (Å) | Continuum Bandpasses (Å) |
|---|---|---|---|
| | *a)* Equivalent Widths | | |
| G 4300 ..... | CH | 4283.25–4317.00 | 4268.25–4283.25<br>4320.75–4335.75 |
| Mg *b* 5177 ..... | Mg *b* | 5162.00–5193.25 | 5144.50–5162.00<br>5193.25–5207.00 |
| Fe 5270 ..... | Fe I, Ca I | 5248.00–5286.75 | 5235.50–5249.25<br>5288.00–5319.25 |
| Fe 5335 ..... | Fe, I, Cr I, Ca I, Ti II | 5314.75–5353.50 | 5307.25–5317.25<br>5356.00–5364.75 |
| Na 5895 ..... | Na D | 5879.25–5910.50 | 5863.00–5876.75<br>5924.50–5949.25 |
| Hβ 4861 ..... | Hβ | 4849.50–4877.00 | 4829.50–4848.25<br>4878.25–4892.00 |
| | *b)* Molecular Bands | | |
| CN ..... | CN | 4144.00–4177.75 | 4082.00–4118.25<br>4246.00–4284.75 |
| $Mg_1$ ..... | MgH | 5071.00–5134.75 | 4897.00–4958.25<br>5303.00–5366.75 |
| $Mg_2$ ..... | MgH + Mg *b* | 5156.00–5197.25 | 4897.00–4958.25<br>5303.00–5366.75 |
| $TiO_1$ ..... | TiO | 5939.00–5995.25 | 5819.00–5850.25<br>6041.00–6104.75 |
| $TiO_2$ ..... | TiO | 6192.00–6273.25 | 6069.00–6142.75<br>6375.00–6416.25 |

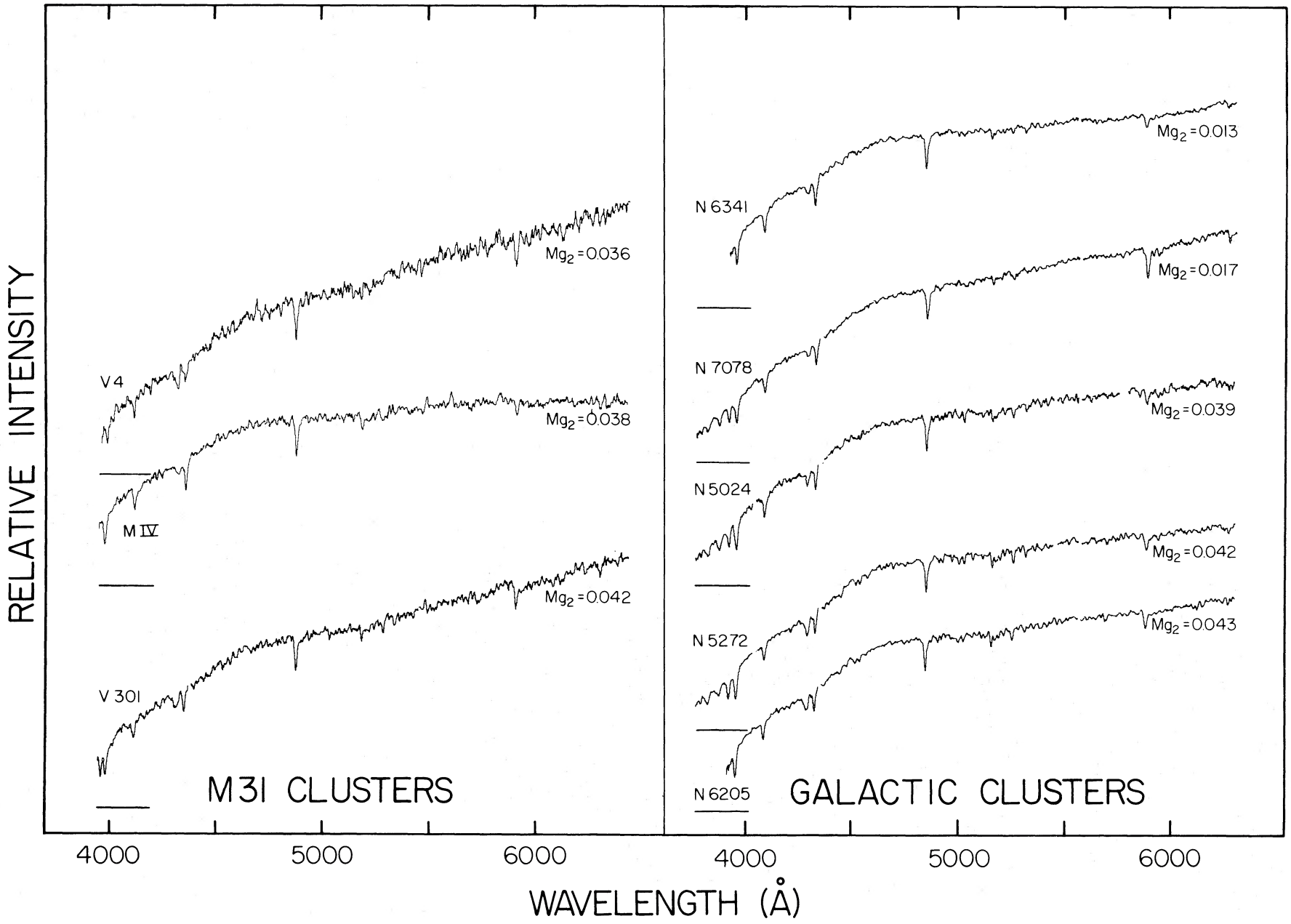


FIG. 1*a*

FIGS. 1*a*–1*d*.—Individual spectra of Galactic and M31 clusters are compared, arranged by increasing line strength. $Mg_2$ is indicated for each object. The step spectra of the metal-rich Galactic clusters and two of the metal-rich M31 clusters are due to high interstellar reddening.

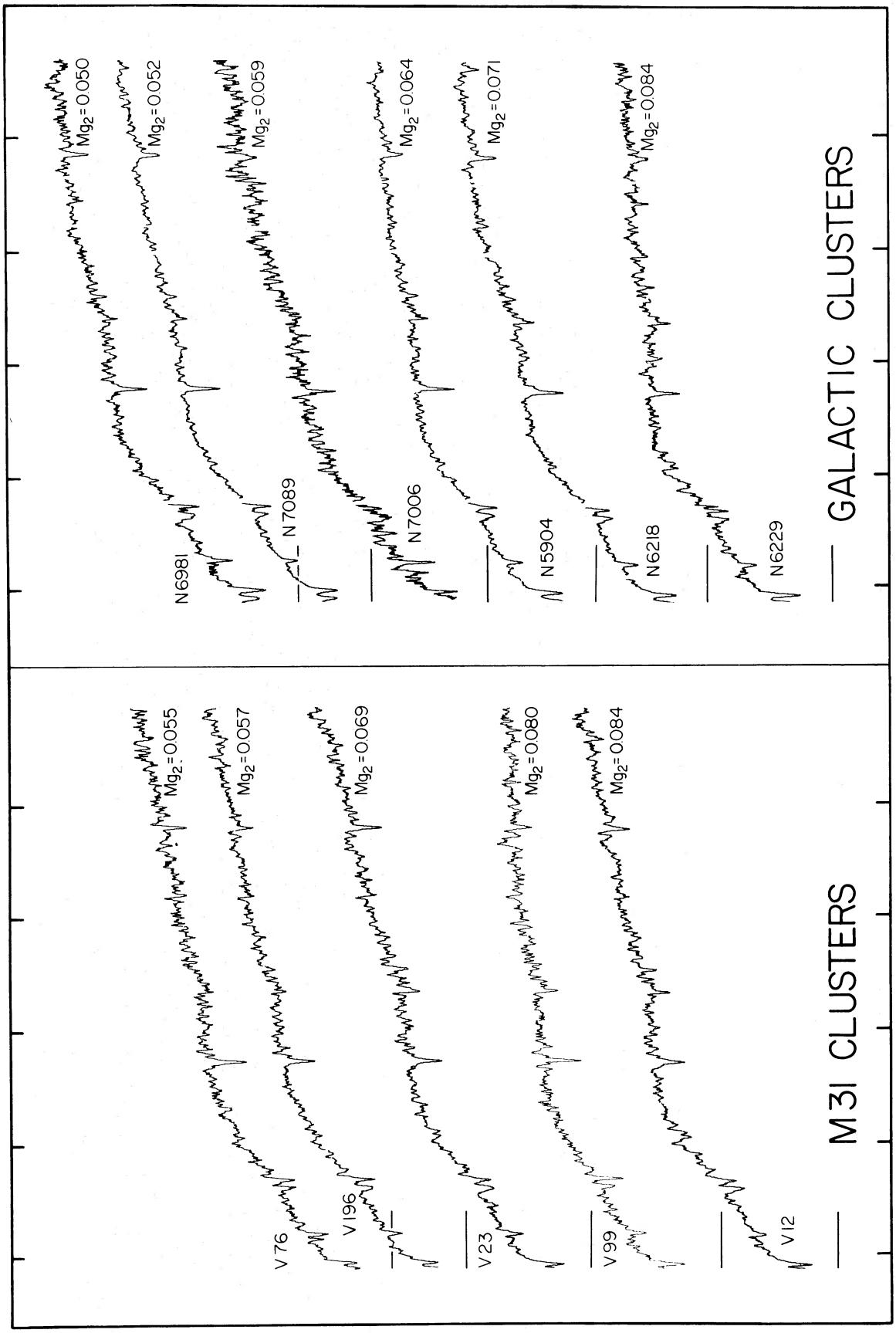


FIG. 1*b*

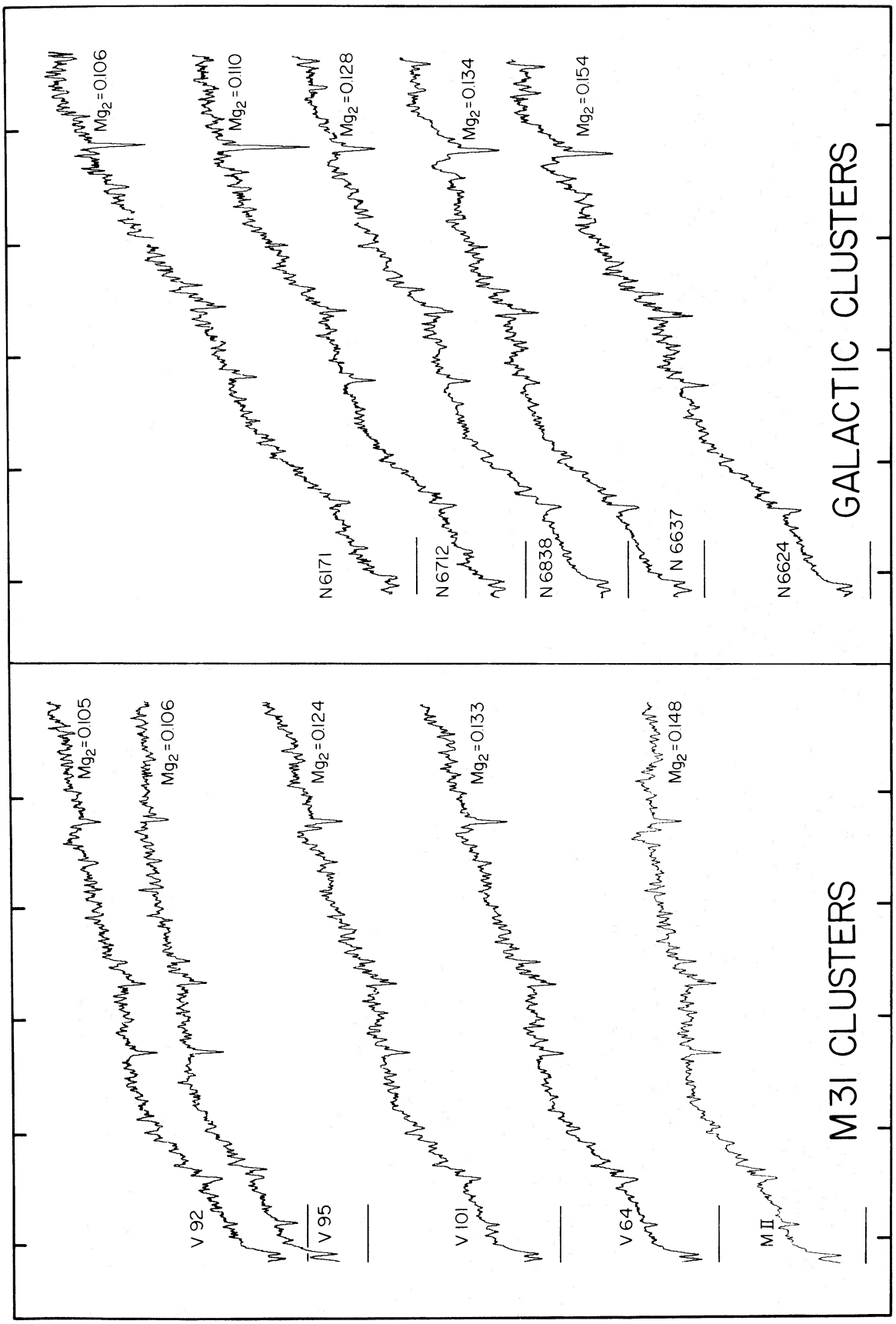


FIG. 1c

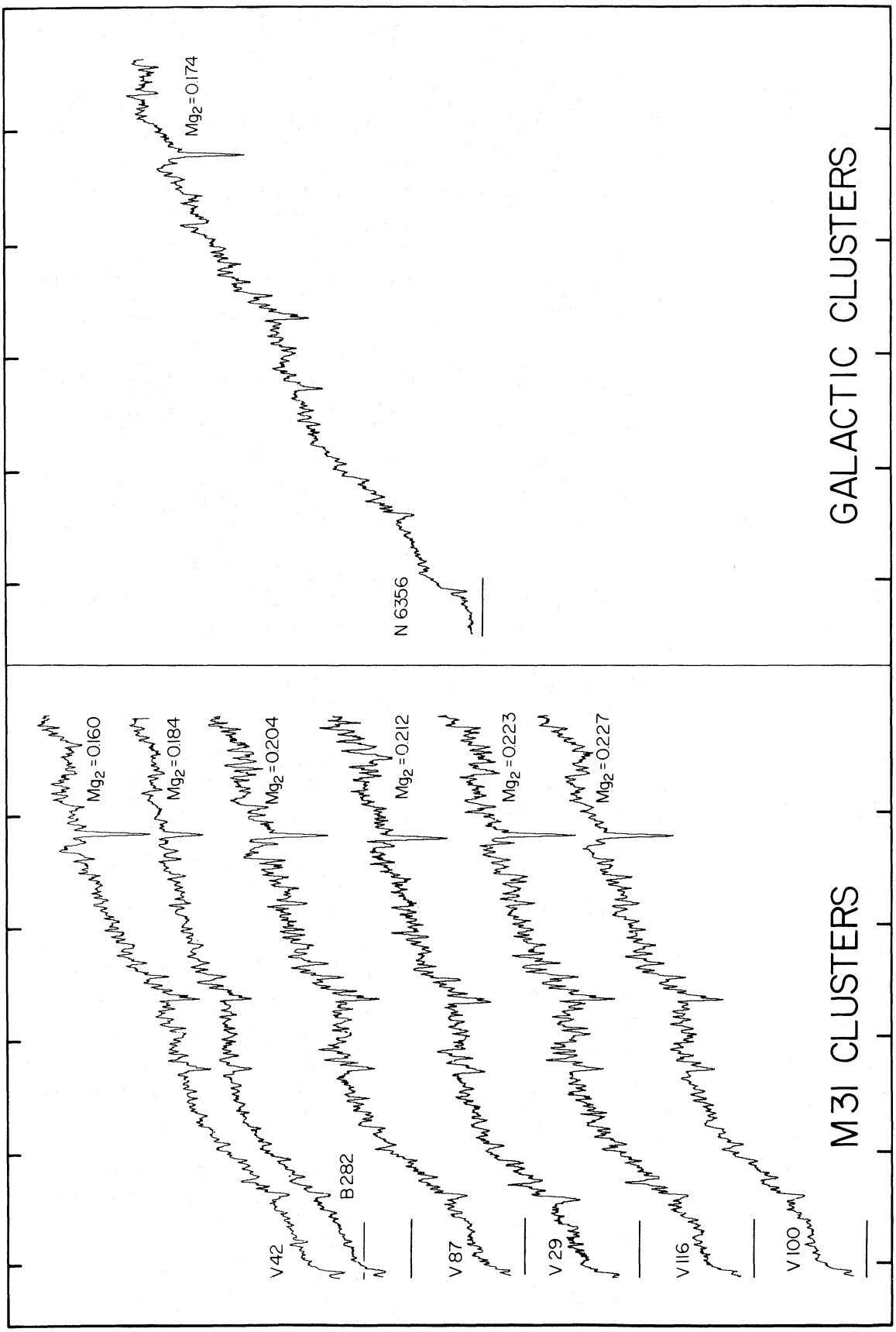


FIG. 1*d*

atomic-line features are expressed in angstroms, and the molecular-band features are expressed as a magnitude ratio: $-2.5$ log (feature/continuum).

Intrinsic inhomogeneity among clusters is potentially important, but good error estimates are needed to assess its presence. Most of the clusters have multiple observations, but the number of observations per cluster is usually only two or three. Independent error estimates therefore exist but are not very accurate. To improve them, we have averaged over all indices in the following way: Let $\sigma_{ij}$ denote the rms error determined from multiple observations of index $i$ for object $j$. Using all objects with multiple measurements, we determined $\bar{\sigma}_i$, the rms error of index $i$ per single observation. Define the quantity

$$S_j = n_j^{-1} \sum_i (\sigma_{ij}/\bar{\sigma}_i) ,$$

where $n_j$ is the number of indices observed for object $j$. $S_j$ is a measure of the accuracy of all data for object $j$. The final adopted error for each index was $S_j \bar{\sigma}_i$. Since this is based on an average over all indices, it is likely to be more accurate than $\sigma_{ij}$ itself. A few objects without multiple observations were assigned error $\bar{\sigma}_i$.

These errors incorporate all random effects but underestimate certain systematic errors due to run-to-run calibration differences or errors in feature placement. For most features these additional effects are small owing to the use of the K giant standard stars and are less than 0.15 Å or 0.01 mag. For the G band the errors are larger, because the upper sideband is contaminated by both H$\gamma$ and Hg $\lambda$4358. When H$\gamma$ is strong, the G band measure can actually become negative, and any error in wavelength placement results in larger-than-average errors. G band errors are also increased by occasional imperfect sky subtraction in Hg $\lambda$4358.

Line indices and errors are given for Galactic clusters in Table 2A and for M31 clusters in Table 2B. Additional data on reddening, colors, assorted metallicity estimates, and absolute magnitudes for these clusters appear in Tables 3A and 3B, with sources as given in the footnotes.

### *b) Metallicity Indicators*

In what follows, an index is needed as a ranking of relative metallicity. Only the Galactic clusters can be used to select such an index, since they are the only objects for which independent metallicity determinations exist. Within the errors, all features are found to correlate well with one another for the Galactic sample. Accordingly, we pick for further investigation that feature which has the highest signal-to-noise ratio, $Mg_2$, plus, for completeness, an average of the two iron-line indices.

Figures 2 and 3 plot these indices against various other metallicity estimators listed in Tables 3A and 3B. Figure 2 shows the broad-band $Q_{39}$ index of Zinn (1980*a*) for Galactic clusters, the $Q_K$ index of Searle for the M31 clusters as quoted by Frogel, Persson, and Cohen (1980), and Kraft's (1979) metallicity estimates, which are a mixture of broad-band estimates and older spectroscopic results. Figure 3 compares the indices with two separate sets of spectroscopically determined metallicities: RR Lyrae $\Delta S$ measurements by Smith and Perkins (1982) and high-resolution spectroscopic analyses of individual cluster giants by Pilachowski, Sneden, and Wallerstein (1983, hereafter PSW). As might be expected from previous discussions of globular cluster metallicities (see PSW for a review), the present low-resolution indices correlate well with other low-resolution data (e.g., Zinn 1980*a*; Smith and Perkins

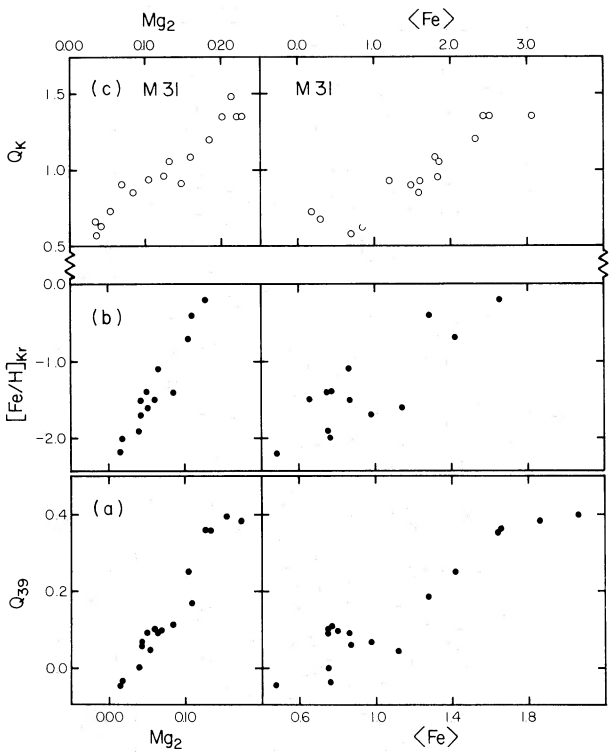


FIG. 2—(*a*) Zinn's (1980*a*) $Q_{39}$ index vs. $Mg_2$ and $\langle Fe \rangle$ for Galactic clusters. [$\langle Fe \rangle \equiv \frac{1}{2}$(Fe 5270 + Fe 5335)]. The scatter in both diagrams is consistent with observational error. (*b*) Kraft's (1979) values of [Fe/H] vs. $Mg_2$ and $\langle Fe \rangle$ for Galactic clusters. The scatter in both diagrams is consistent with observational error. (*c*) Searle's $Q_K$ vs. $Mg_2$ and $\langle Fe \rangle$ for M31 clusters.

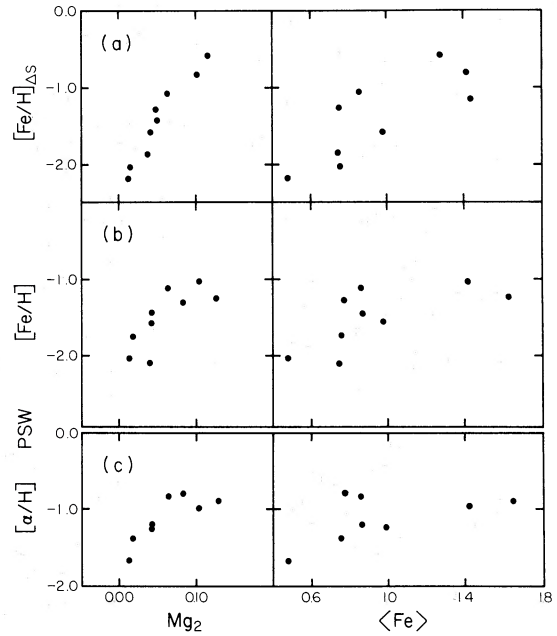


FIG. 3.—(*a*) RR Lyrae $\Delta S$ metallicities by Smith and Perkins (1982) vs. $Mg_2$ and $\langle Fe \rangle$ for Galactic clusters. (*b*) High-dispersion spectroscopic metallicities by PSW vs. $Mg_2$ and $\langle Fe \rangle$ for Galactic clusters. Note the higher scatter and departure from linearity at high line strengths, in contrast to Figs. 2*a*–2*c* and 3*a* above. (*c*) Alpha-process abundances by PSW vs. $Mg_2$ and $\langle Fe \rangle$ for Galactic clusters. Note the higher scatter and departure from linearity at high line strengths, in contrast to Figs. 2*a*–2*c* and 3*a* above.

TABLE 2A

LINE INDICES FOR GALACTIC GLOBULAR CLUSTERS

| Name | No. Obs. | G 4300 | Mg *b* 5177 | Fe 5270 | Fe 5335 | Na 5895 | H$\beta$ 4861 | CN | $Mg_1$ | $Mg_2$ | $TiO_1$ | $TiO_2$ |
|---|---|---|---|---|---|---|---|---|---|---|---|---|
| N5024 = M53 ..... | 1 | 1.12 | 0.70 | 0.65 | 0.85 | 0.47 | 2.74 | −0.127 | 0.002 | 0.039 | 0.015 | ... |
| | | ±0.46 | ±0.16 | ±0.24 | ±0.14 | ±0.27 | ±0.22 | ±0.016 | ±0.008 | ±0.011 | ±0.006 | ... |
| N5272 = M3 ..... | 1 | 2.26 | 0.76 | 1.15 | 0.80 | 1.07 | 2.44 | −0.079 | −0.002 | 0.042 | 0.002 | ... |
| | | ±0.34 | ±0.12 | ±0.18 | ±0.10 | ±0.20 | ±0.16 | ±0.012 | ±0.006 | ±0.008 | ±0.004 | ... |
| N5904 = M5 ..... | 1 | 2.16 | 1.04 | 1.20 | 0.52 | 1.15 | 2.29 | −0.085 | 0.012 | 0.064 | 0.016 | ... |
| | | ±0.24 | ±0.08 | ±0.13 | ±0.07 | ±0.14 | ±0.11 | ±0.008 | ±0.004 | ±0.006 | ±0.003 | ... |
| N6171 ..... | 1 | 3.48 | 1.84 | 1.96 | 0.88 | 1.85 | 1.48 | −0.107 | 0.021 | 0.106 | 0.006 | ... |
| | | ±0.57 | ±0.20 | ±0.30 | ±0.17 | ±0.33 | ±0.27 | ±0.020 | ±0.010 | ±0.013 | ±0.007 | ... |
| N6205 = M13 ..... | 1 | 1.85 | 0.78 | 0.94 | 0.79 | 1.04 | 2.25 | −0.085 | 0.000 | 0.043 | 0.006 | ... |
| | | ±0.17 | ±0.06 | ±0.09 | ±0.05 | ±0.10 | ±0.08 | ±0.006 | ±0.003 | ±0.004 | ±0.002 | ... |
| N6218 ..... | 1 | 2.26 | 1.43 | 1.16 | 0.44 | 1.41 | 2.55 | −0.096 | 0.011 | 0.071 | 0.012 | ... |
| | | ±0.37 | ±0.13 | ±0.19 | ±0.11 | ±0.22 | ±0.18 | ±0.013 | ±0.006 | ±0.009 | ±0.005 | ... |
| N6229 ..... | 1 | 1.86 | 1.34 | 1.01 | 0.52 | 1.12 | 2.06 | −0.094 | 0.012 | 0.084 | −0.006 | ... |
| | | ±0.65 | ±0.23 | ±0.34 | ±0.20 | ±0.38 | ±0.31 | ±0.023 | ±0.011 | ±0.015 | ±0.008 | ... |
| N6341 = M92 ..... | 2 | 0.49 | 0.68 | 0.25 | 0.70 | 0.94 | 2.57 | −0.099 | −0.012 | 0.013 | 0.003 | −0.014 |
| | | ±0.20 | ±0.07 | ±0.11 | ±0.06 | ±0.12 | ±0.10 | ±0.007 | ±0.003 | ±0.005 | ±0.003 | ±0.005 |
| N6356 ..... | 2 | 4.52 | 2.99 | 2.03 | 1.68 | 3.20 | 1.47 | 0.015 | 0.058 | 0.174 | 0.044 | 0.048 |
| | | ±0.49 | ±0.17 | ±0.26 | ±0.15 | ±0.29 | ±0.24 | ±0.017 | ±0.008 | ±0.011 | ±0.006 | ±0.004 |
| N6624 ..... | 3 | 4.75 | 2.62 | 2.17 | 1.97 | 2.88 | 1.74 | 0.020 | 0.053 | 0.154 | 0.051 | 0.063 |
| | | ±0.37 | ±0.13 | ±0.19 | ±0.11 | ±0.22 | ±0.18 | ±0.013 | ±0.006 | ±0.009 | ±0.005 | ±0.003 |
| N6637 = M69 ..... | 2 | 5.16 | 2.20 | 2.12 | 1.17 | 3.09 | 1.15 | −0.008 | 0.045 | 0.134 | 0.054 | ... |
| | | ±0.51 | ±0.18 | ±0.26 | ±0.15 | ±0.30 | ±0.24 | ±0.018 | ±0.009 | ±0.012 | ±0.007 | ... |
| N6712 ..... | 1 | 2.56 | 1.56 | 1.45 | 1.10 | 4.01 | 1.82 | −0.053 | 0.054 | 0.110 | −0.001 | ... |
| | | ±0.39 | ±0.13 | ±0.20 | ±0.12 | ±0.23 | ±0.18 | ±0.013 | ±0.007 | ±0.009 | ±0.005 | ... |
| N6838 = M71 ..... | 2 | 5.20 | 2.26 | 1.46 | 1.83 | 1.92 | 1.43 | −0.017 | 0.052 | 0.128 | 0.034 | 0.026 |
| | | ±0.75 | ±0.26 | ±0.39 | ±0.23 | ±0.44 | ±0.36 | ±0.026 | ±0.013 | ±0.018 | ±0.010 | ±0.006 |
| N6981 = M72 ..... | 1 | 0.97 | 0.70 | 0.86 | 0.63 | 1.54 | 2.33 | −0.069 | 0.014 | 0.050 | 0.007 | ... |
| | | ±0.58 | ±0.20 | ±0.30 | ±0.18 | ±0.34 | ±0.28 | ±0.020 | ±0.010 | ±0.014 | ±0.008 | ... |
| N7006 ..... | 1 | 3.36 | 0.47 | 0.51 | 0.79 | 1.78 | 2.38 | −0.054 | 0.034 | 0.059 | 0.003 | ... |
| | | ±0.69 | ±0.24 | ±0.36 | ±0.21 | ±0.40 | ±0.33 | ±0.024 | ±0.012 | ±0.016 | ±0.009 | ... |
| N7078 = M15 ..... | 1 | 0.68 | 0.32 | 0.98 | 0.54 | 1.88 | 2.53 | −0.102 | −0.005 | 0.017 | 0.011 | ... |
| | | ±0.28 | ±0.10 | ±0.14 | ±0.08 | ±0.16 | ±0.13 | ±0.010 | ±0.005 | ±0.007 | ±0.004 | ... |
| N7089 = M2 ..... | 1 | 1.73 | 0.89 | 1.09 | 1.18 | 1.28 | 2.55 | −0.079 | 0.002 | 0.052 | 0.003 | ... |
| | | ±0.23 | ±0.08 | ±0.12 | ±0.07 | ±0.13 | ±0.11 | ±0.008 | ±0.004 | ±0.005 | ±0.003 | ... |

TABLE 2B

LINE INDICES FOR M31 GLOBULAR CLUSTERS

| Name | No. Obs. | G 4300 | Mg *b* 5177 | Fe 5270 | Fe 5335 | Na 5895 | Hβ 4861 | CN | $Mg_1$ | $Mg_2$ | $TiO_1$ | $TiO_2$ |
|---|---|---|---|---|---|---|---|---|---|---|---|---|
| M II = K1 ..... | 1 | 3.65 | 2.24 | 1.78 | 1.44 | 2.13 | 2.38 | 0.025 | 0.049 | 0.148 | 0.032 | 0.029 |
| | | ±0.47 | ±0.23 | ±0.31 | ±0.31 | ±0.31 | ±0.25 | ±0.014 | ±0.011 | ±0.007 | ±0.009 | ±0.005 |
| M IV = K219 ..... | 1 | 0.42 | 0.66 | 0.95 | 0.47 | 1.24 | 2.71 | −0.050 | 0.006 | 0.038 | 0.022 | −0.001 |
| | | ±0.49 | ±0.25 | ±0.32 | ±0.33 | ±0.33 | ±0.27 | ±0.014 | ±0.011 | ±0.008 | ±0.010 | ±0.005 |
| V4 = K33 ..... | 1 | 2.89 | −0.44 | −0.02 | 0.68 | 1.57 | 2.95 | −0.073 | 0.007 | 0.036 | −0.001 | −0.015 |
| | | ±0.47 | ±0.23 | ±0.31 | ±0.31 | ±0.31 | ±0.25 | ±0.014 | ±0.011 | ±0.007 | ±0.009 | ±0.005 |
| V12 = K76[a] ..... | 1 | 3.07 | 1.38 | 1.60 | 1.57 | 1.23 | 2.16 | −0.026 | 0.026 | 0.084 | 0.023 | 0.013 |
| | | ±0.52 | ±0.26 | ±0.34 | ±0.35 | ±0.35 | ±0.28 | ±0.015 | ±0.012 | ±0.008 | ±0.010 | ±0.005 |
| V23 = K119[a] ..... | 1 | 2.88 | 1.95 | 1.86 | 1.07 | 1.99 | 2.21 | −0.036 | 0.017 | 0.069 | 0.012 | 0.020 |
| | | ±0.52 | ±0.26 | ±0.34 | ±0.35 | ±0.35 | ±0.28 | ±0.015 | ±0.012 | ±0.008 | ±0.010 | ±0.005 |
| V29 = K90[a] ..... | 1 | 7.46[b] | 4.47[b] | 1.89[b] | 0.92[b] | 2.93[b] | 1.61[b] | 0.117 | 0.087 | 0.212 | 0.031 | 0.068 |
| | | ... | ... | ... | ... | ... | ... | ±0.019 | ±0.015 | ±0.011 | ±0.013 | ±0.006 |
| V42 = K78 ..... | 1 | 4.41 | 2.61 | 1.96 | 1.61 | 3.83 | 2.10 | 0.021 | 0.041 | 0.160 | 0.026 | 0.050 |
| | | ±0.42 | ±0.21 | ±0.27 | ±0.28 | ±0.28 | ±0.22 | ±0.012 | ±0.010 | ±0.006 | ±0.008 | ±0.004 |
| V64 = K213[a] ..... | 1 | 4.13 | 2.40 | 2.00 | 1.71 | 2.57 | 1.92 | 0.004 | 0.047 | 0.133 | 0.010 | 0.031 |
| | | ±0.52 | ±0.26 | ±0.34 | ±0.35 | ±0.35 | ±0.28 | ±0.015 | ±0.012 | ±0.008 | ±0.010 | ±0.005 |
| V76 = K263 ..... | 1 | 1.73 | 0.53 | −0.30 | 0.67 | 0.84 | 3.06 | −0.072 | 0.015 | 0.055 | 0.010 | −0.020 |
| | | ±0.38 | ±0.19 | ±0.25 | ±0.26 | ±0.26 | ±0.20 | ±0.011 | ±0.009 | ±0.006 | ±0.007 | ±0.004 |
| V87 = K222 ..... | 1 | 4.27 | 2.98 | 2.33 | 2.52 | 4.01 | 2.37 | 0.114 | 0.084 | 0.201 | 0.039 | 0.043 |
| | | ±0.77 | ±0.38 | ±0.50 | ±0.52 | ±0.52 | ±0.41 | ±0.022 | ±0.018 | ±0.012 | ±0.015 | ±0.007 |
| V92 = K230[a] ..... | 1 | 4.51 | 1.78 | 1.56 | 0.82 | 1.41 | 1.82 | −0.020 | 0.027 | 0.105 | 0.019 | 0.012 |
| | | ±0.52 | ±0.26 | ±0.34 | ±0.35 | ±0.35 | ±0.28 | ±0.015 | ±0.012 | ±0.008 | ±0.010 | ±0.005 |
| V95 = K229 ..... | 1 | 1.04 | 1.93 | 2.08 | 0.54 | 1.40 | 2.41 | −0.061 | 0.032 | 0.106 | 0.012 | −0.003 |
| | | ±0.29 | ±0.15 | ±0.19 | ±0.20 | ±0.20 | ±0.16 | ±0.008 | ±0.007 | ±0.004 | ±0.006 | ±0.003 |
| V99 = K286 ..... | 1 | 1.91 | 1.49 | 0.97 | 0.46 | 1.42 | 2.72 | −0.069 | 0.008 | 0.081 | 0.035 | 0.007 |
| | | ±0.79 | ±0.40 | ±0.52 | ±0.53 | ±0.53 | ±0.43 | ±0.023 | ±0.018 | ±0.012 | ±0.015 | ±0.008 |
| V100 = K217 ..... | 2 | 5.10 | 3.68 | 2.60 | 2.39 | 4.07 | 1.66 | 0.124 | 0.088 | 0.227 | 0.042 | 0.071 |
| | | ±0.20 | ±0.68 | ±0.17 | ±0.16 | ±0.23 | ±0.10 | ±0.019 | ±0.004 | ±0.008 | ±0.010 | ±0.010 |
| V101 = K272[a] ..... | 1 | 3.89 | 2.40 | 1.94 | 1.72 | 1.68 | 1.94 | −0.010 | 0.046 | 0.124 | 0.037 | 0.033 |
| | | ±0.52 | ±0.26 | ±0.34 | ±0.35 | ±0.35 | ±0.28 | ±0.015 | ±0.012 | ±0.008 | ±0.010 | ±0.005 |
| V116 = K244 ..... | 1 | 3.98 | 3.16 | 3.30 | 2.87 | 4.60 | 2.19 | 0.155 | 0.076 | 0.223 | 0.026 | 0.064 |
| | | ±0.40 | ±0.20 | ±0.26 | ±0.27 | ±0.27 | ±0.21 | ±0.012 | ±0.010 | ±0.006 | ±0.008 | ±0.004 |
| V196 = K302 ..... | 2 | 2.58 | 0.60 | 0.64 | 0.95 | 1.11 | 2.08 | −0.031 | 0.022 | 0.057 | 0.010 | 0.012 |
| | | ±0.13 | ±0.55 | ±0.26 | ±0.20 | ±0.44 | ±0.20 | ±0.022 | ±0.007 | ±0.003 | ±0.010 | ±0.005 |
| B282 = K280 ..... | 2 | 5.18 | 3.12 | 2.63 | 2.00 | 2.91 | 2.19 | 0.072 | 0.049 | 0.184 | 0.032 | 0.041 |
| | | ±0.68 | ±0.34 | ±0.45 | ±0.46 | ±0.46 | ±0.37 | ±0.020 | ±0.016 | ±0.010 | ±0.013 | ±0.007 |
| V301 = K64[a] ..... | 1 | 2.14 | 0.88 | 1.04 | 0.63 | 1.58 | 2.51 | −0.039 | 0.012 | 0.042 | 0.001 | −0.009 |
| | | ±0.52 | ±0.26 | ±0.34 | ±0.35 | ±0.35 | ±0.28 | ±0.015 | ±0.012 | ±0.008 | ±0.010 | ±0.005 |

[a] Mean errors from the other 12 clusters assigned to these clusters.
[b] Low-resolution spectrum; only molecular-band measures are valid.

TABLE 3A

OTHER DATA FOR GALACTIC GLOBULAR CLUSTERS

| Name | $E(B-V)$[a] | $(B-V)_0$[b] | $(U-V)_0$[b] | $(V-K)_0$[c] | $(J-K)_0$[c] | $Q_{39}$[d] | [Fe/H] $\Delta S$[e] | $[Fe/H]_{PSW}$ $[\alpha/H]_{PSW}$[f] | $[Fe/H]_{Kr}$[g] | $M_V$[h] | $Mg_2$ |
|---|---|---|---|---|---|---|---|---|---|---|---|
| N5024 ..... | 0.00 | 0.64 | 0.74 | 2.15 | 0.61 | −0.002 | −1.85 | −2.10 | −1.9 | −8.5 | 0.039 |
| N5272 ..... | 0.01 | 0.68 | 0.77 | 2.13 | 0.62 | 0.066 | −1.57 | −1.57 | −1.7 | −8.7 | 0.042 |
| | | | | | | | | −1.23 | | | |
| N5904 ..... | 0.03 | 0.68 | 0.78 | 2.31 | 0.69 | 0.090 | −1.08 | −1.13 | −1.1 | −8.8 | 0.064 |
| | | | | | | | | −0.83 | | | |
| N6171 ..... | 0.30 | 0.84 | 1.15 | 2.86 | 0.79 | 0.247 | −0.83 | −1.05 | −0.7 | −6.7 | 0.106 |
| | | | | | | | | −0.98 | | | |
| N6205 ..... | 0.02 | 0.67 | 0.68 | 2.44 | 0.67 | 0.057 | ... | −1.44 | −1.5 | −8.5 | 0.043 |
| | | | | | | | | −1.19 | | | |
| N6218 ..... | 0.17 | 0.65 | 0.72 | 2.11 | 0.65 | 0.096 | ... | ... | ... | −7.6 | 0.071 |
| N6229 ..... | 0.02 | 0.69 | 0.72: | 2.36 | 0.66 | 0.112 | ... | −1.30 | −1.4 | −8.1 | 0.084 |
| | | | | | | | | −0.80 | | | |
| N6341 ..... | 0.02 | 0.60 | 0.58 | 2.14 | 0.59 | −0.047 | −2.18 | −2.06 | −2.2 | −8.0 | 0.013 |
| | | | | | | | | −1.68 | | | |
| N6356 ..... | 0.4: | 0.71: | 0.99: | 2.52: | 0.78: | 0.385 | ... | ... | ... | −9.0 | 0.174 |
| N6624 ..... | 0.33: | 0.70: | 0.95: | 2.69: | 0.85: | 0.397 | ... | ... | ... | −7.4 | 0.154 |
| N6637 ..... | 0.20 | 0.79 | 1.13 | 2.59 | 0.83 | 0.362 | ... | ... | ... | −8.0 | 0.134 |
| N6712 ..... | 0.48 | 0.68 | 0.84 | 2.32 | 0.77 | 0.184 | −0.57 | ... | −0.4 | −7.7 | 0.110 |
| N6838 ..... | 0.27 | 0.86 | 1.18 | 2.68 | 0.78 | 0.359 | ... | −1.25 | −0.2 | −5.6 | 0.128 |
| | | | | | | | | −0.90 | | | |
| N6981 ..... | 0.07 | 0.65 | 0.73 | 2.22 | 0.70 | 0.091 | −1.27 | ... | −1.4 | −7.1 | 0.050 |
| N7006 ..... | 0.10 | 0.64 | 0.73 | 2.10 | 0.54 | 0.101 | ... | ... | −1.5 | −7.4 | 0.059 |
| N7078 ..... | 0.12 | 0.56 | 0.52 | 1.80 | 0.56 | −0.038 | −2.04 | −1.76 | −2.0 | −8.9 | 0.017 |
| | | | | | | | | −1.37 | | | |
| N7089 ..... | 0.06 | 0.61 | 0.65 | 2.19 | 0.64 | 0.044 | −1.43 | ... | −1.6 | −9.0 | 0.052 |

[a] From Burstein and McDonald 1975 and Burstein and Heiles 1978; value for N6624 is mean value from Liller and Liller 1976.
[b] Raw values from Harris and Racine 1979; $E(U-B) = 0.75E(B-V)$.
[c] Raw values from Aaronson and Malkan 1983; $E(V-K) = 2.8E(B-V)$; $E(J-K) = 0.5E(B-V)$.
[d] From Zinn 1980*a*.
[e] From RR Lyrae stars by Smith and Perkins 1982.
[f] Pilachowski, Sneden, and Wallerstein 1983.
[g] Kraft 1979.
[h] From Harris and Racine 1979, adjusted to reddenings used here.

TABLE 3B

OTHER DATA FOR M31 GLOBULAR CLUSTERS

| Name | $E(B-V)$[a] | $(B-V)_0$[b] | $(U-V)_0$[b] | $(V-K)_0$[b] | $(J-K)_0$[b] | $Q_K$[c] | $M_V$[d] | $Mg_2$ |
|---|---|---|---|---|---|---|---|---|
| M II ..... | 0.08 | 0.78 | 1.01 | 2.44 | 0.76 | 0.92 | −10.7 | 0.148 |
| M IV ..... | 0.08 | 0.58 | 0.51 | 1.93 | 0.62 | 0.57 | −9.3 | 0.038 |
| V4 ..... | 0.20 | 0.71 | 0.66 | 2.11 | 0.61 | 0.67 | −9.3 | 0.036 |
| V12 ..... | 0.08 | 0.64 | 0.91 | 2.42 | 0.70 | 0.85 | −10.1 | 0.084 |
| V23 ..... | 0.08 | 0.75 | 0.88 | 2.41 | 0.67 | 0.89 | −9.4 | 0.069 |
| V29 ..... | 0.08: | 1.09: | 1.64: | 3.14: | 0.98: | 1.47 | −7.9 | 0.212 |
| V42 ..... | 0.29 | 0.83 | 1.12 | 2.71 | 0.75 | 1.08 | −10.8 | 0.160 |
| V64 ..... | 0.08 | 0.82 | 1.08 | 2.61 | 0.76 | 1.05 | −9.7 | 0.133 |
| V76 ..... | 0.08 | 0.58 | 0.57 | 2.21 | 0.65 | 0.73 | −8.8 | 0.055 |
| V87 ..... | 0.08 | 0.90 | 1.39 | 2.89 | 0.84 | 1.35 | −9.2 | 0.201 |
| V92 ..... | 0.08 | 0.74 | 0.94 | 2.28 | 0.75 | 0.93 | −9.2 | 0.105 |
| V95 ..... | 0.08 | 0.68 | 0.72 | ... | ... | ... | −9.4 | 0.106 |
| V99 ..... | 0.08 | 0.69 | 0.74 | ... | ... | ... | −8.7 | 0.081 |
| V100 ..... | 0.16 | 0.95 | 1.40 | 2.97 | 0.87 | 1.35 | −9.6 | 0.227 |
| V101 ..... | 0.08 | 0.76 | 1.00 | 2.62 | 0.78 | 0.94 | −9.7 | 0.124 |
| V116 ..... | 0.08 | 0.91 | 1.56 | 2.96 | 0.84 | 1.36 | −9.0 | 0.223 |
| V196 ..... | 0.08 | 0.67 | 0.69 | 2.11 | 0.67 | ... | −9.2 | 0.057 |
| V282 ..... | 0.08 | 0.84 | 1.25 | 2.89 | 0.84 | 1.20 | −10.2 | 0.184 |
| V301 ..... | 0.16 | 0.61 | 0.62 | 2.00 | 0.54 | 0.63 | −9.5 | 0.042 |

[a] A foreground reddening of $E(B-V) = 0.08$ is assumed for M31 (Burstein and Heiles 1982); values in excess of this are estimates of Searle, as quoted in Frogel, Persson, and Cohen 1980.
[b] Raw values from Frogel, Persson, and Cohen 1980 or van den Bergh 1969.
[c] From Searle, as quoted in Frogel, Persson, and Cohen 1980.
[d] $(m-M)_0 = 24.13$ for M31; $V$-magnitudes from Frogel, Persson, and Cohen 1980 or van den Bergh 1969.

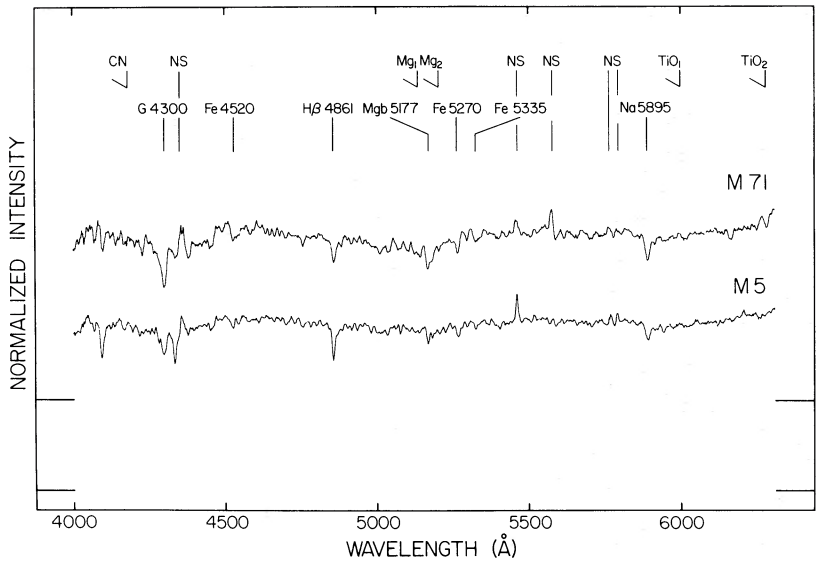


FIG. 4.—Spectra of M71 (NGC 6838) and M5 (NGC 5904), flattened by division with a fifth-order polynomial curve to aid the comparison of relative absorption-line strengths. Despite their similar high-resolution spectroscopic metallicities, as quoted by PSW, the two clusters look very different in these moderate-resolution spectra. Stronger absorption lines are visible at all wavelengths in M71, including λ4520 of Searle and Zinn (1978) and $Mg_2$.

1982) but poorly with the high-resolution results of PSW, especially for the most metal-rich clusters. The curvature and scatter in the present indices compared with those of PSW are not appreciably alleviated by plotting them against PSW's α-peak abundances instead of iron (see Fig. 3*c*).

Possible reasons for these differences have been fully reviewed by PSW. We add only one point to their discussion, concerning M5 and M71. According to PSW and Peterson (1981), these two clusters have nearly equal [Fe/H] values (near −1.2) yet exhibit very different low-resolution indices. The latter fact is confirmed in our spectra, which are shown for reference in Figure 4. Essentially all features visible at this resolution are stronger in M71 than in M5 (cf. also Rabin 1980). This difference also agrees with IDS spectra of individual giant-branch stars in both clusters (Zinn 1984; Burstein *et al.* 1985). Note particularly that the 4520 Å iron-peak complex measured by Searle and Zinn (1978) is as much enhanced in M71 as the bulk of the lines. PSW laid great stress on the fact that Searle and Zinn's (1978) index showed no difference between the two clusters, but in view of the way the index is defined, no difference should be expected, owing to spectral curvature (R. Zinn, private communication). In short, we feel that, at low resolution, M5 and M71 continue to look very different at all wavelengths, not just in the ultraviolet as PSW believed, and that the discrepancy between the high- and low-resolution studies of these two clusters still remains.

Since no consensus on a definitive metallicity scale for Galactic clusters has yet emerged, the best we can do here is to use that feature which has the highest signal-to-noise ratio, namely, $Mg_2$. On the other hand, $Mg_2$ is also sensitive to differences in age, CNO abundance, and hot stellar content (see § IV*a*). If these other factors vary, $Mg_2$ may not correlate uniquely with metallicity, and detailed spectral modeling may be necessary.

### *c*) *Absorption-Line Indices*

In Figures 5*a*–5*l* the remaining line indices are plotted against $Mg_2$, and the behavior of Galactic globulars, M31 globulars, and the nuclei of normal E galaxies are intercompared. The mean least squares relationships for 170 E and E/S0 galaxy nuclei versus $Mg_2$ are shown as straight lines, with the rms scatter of a typical point indicated by the crossbar. All galaxy data have been corrected for velocity broadening (Faber *et al.* 1984*b*) and refer to an aperture size of 1.″4 × 4.″0.

#### i) *"Normal" Line Indices:* G *Band,* Mg *b,* Fe, $Mg_1$, *and* TiO

The line indices measured here can be divided into two groups. In the first, or "normal," group, there is no difference in behavior between the two cluster samples and no visible discontinuity between clusters on the one hand and galaxies on the other. Most features belong to this group, including the G band, both iron lines, both TiO bands, Mg *b*, and $Mg_1$ (the MgH measure) (Figs. 5*a*–5*h*). This is the behavior expected under the simple assumption that all three stellar populations are basically similar to one another save for metallicity.

Although no discontinuities are evident in the normal group, the G band and the iron lines do show a pronounced flattening of slope near $Mg_2 = 0.20$ mag, the boundary between clusters and galaxies. The net result is that, among the galaxies themselves, features like Mg *b* and MgH (and Na and CN) show large variations, whereas changes in the G band and iron are barely detectable. This near-constancy of the G band is consistent with stellar studies (Faber *et al.* 1984*a*), which show that this feature exhibits little variation in temperature or metallicity for K giants above [Fe/H] = −0.5. The lack of a significant change in iron is harder to understand, however, since both Fe λ5270 and Fe λ5335 vary strongly with temperature and abundance in K giants. Perhaps the iron difference between dwarf and giant ellipticals is actually much less than has traditionally been thought (e.g., Faber 1973*a*; Burstein 1979; Cohen 1979), but, if so, the large changes in $Mg_2$ and other features then become quite mysterious. Working out the relative changes between iron and the other lines is one of the major aims of a semitheoretical synthesis of E galaxy spectra that is currently in progress.

#### ii) Na D: *Interstellar Absorption*

The Na D feature (Fig. 5*i*) presents a special problem because of possible contamination by interstellar lines. Although significant population differences appear in Figure

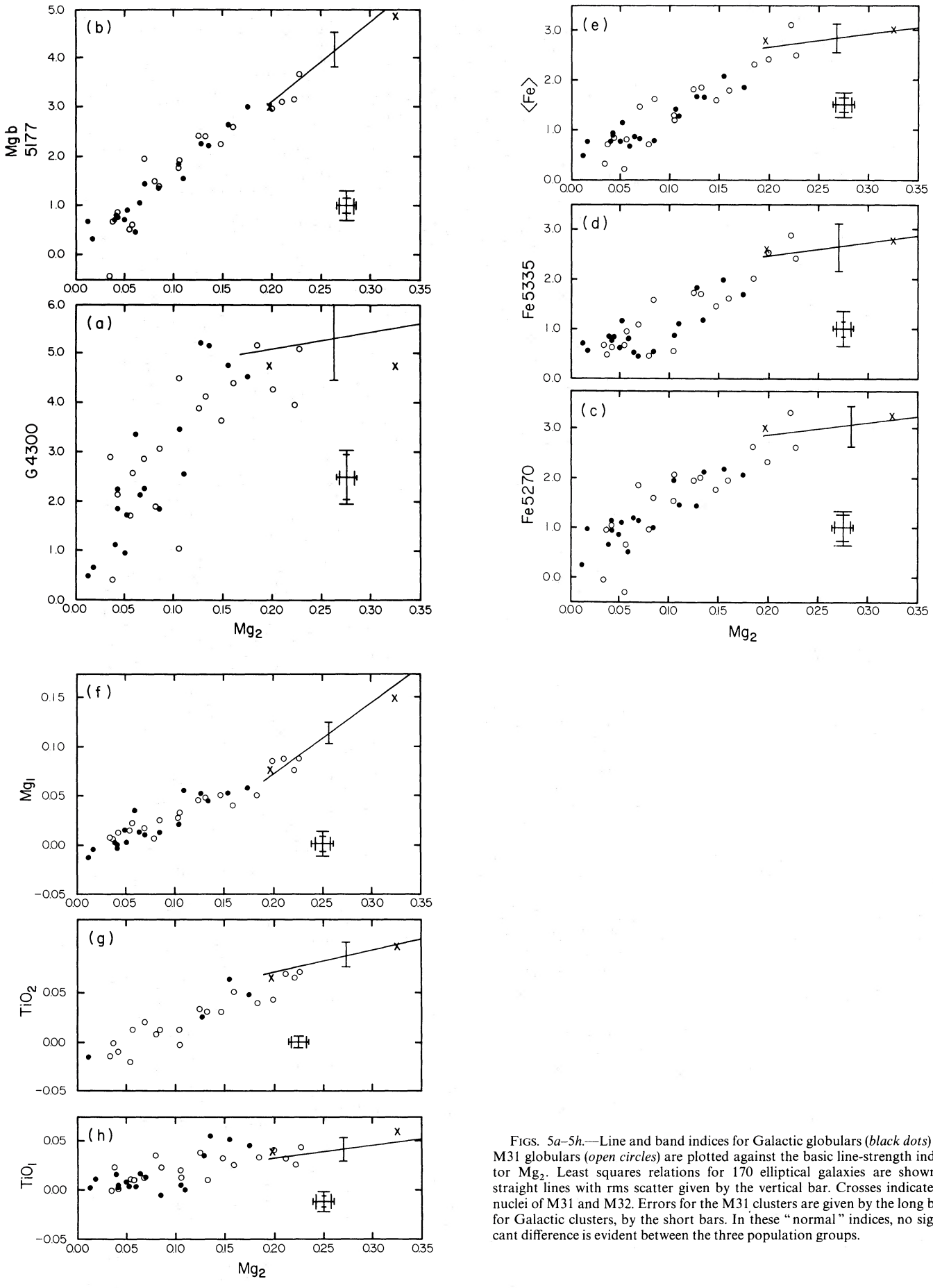


FIGS. 5*a*–5*h*.—Line and band indices for Galactic globulars (*black dots*) and M31 globulars (*open circles*) are plotted against the basic line-strength indicator $Mg_2$. Least squares relations for 170 elliptical galaxies are shown as straight lines with rms scatter given by the vertical bar. Crosses indicate the nuclei of M31 and M32. Errors for the M31 clusters are given by the long bars; for Galactic clusters, by the short bars. In these "normal" indices, no significant difference is evident between the three population groups.

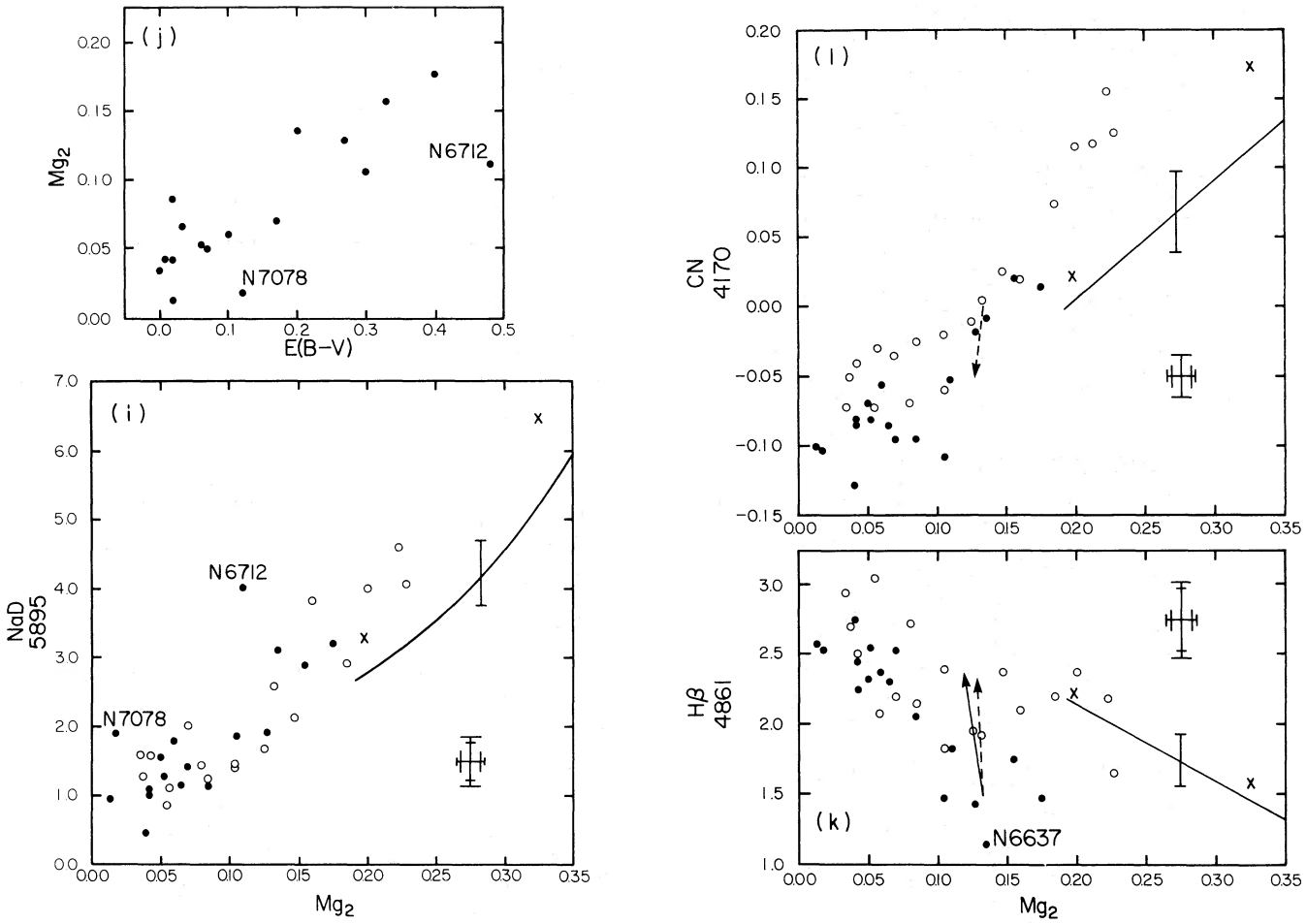


FIGS. 5*i*–5*l*.—(*i*) Same as Figs. 5*a*–5*h*, for Na D. Both cluster groups are systematically offset from the galaxies, and a few individual clusters deviate even farther from the mean trends. A possible explanation is contamination by interstellar Na D absorption (see text). (*j*) $Mg_2$ vs. $E(B-V)$ for Galactic clusters. Deviant points are labeled. Along with Fig. 5*i*, the graph illustrates the impossibility of separating interstellar absorption from true Na D width among the Galactic clusters from these line and color data alone. (*k*) Same as Figs. 5*a*–5*h*, for H$\beta$. Above the level $Mg_2 = 0.10$, both M31 clusters and elliptical galaxies are systematically offset in H$\beta$ above the Galactic globulars. The effect of substituting a blue horizontal branch in M71 or 47 Tuc is shown by the dashed arrow (see Table 5). The effect of viewing these clusters at younger age ($5 \times 10^9$ yr) is shown by the solid arrow (see Table 5). (*l*) Same as Figs. 5*a*–5*h*, for CN. Several M31 clusters are systematically offset to higher CN values with respect to both the Galactic clusters and elliptical galaxies (see text). The arrow is as in Fig. 5*k*.

5*i*, these differences could be spurious owing to interstellar absorption. Almost all Galactic globular clusters are reddened to some degree, and all of the M31 clusters are significantly reddened by Galactic dust plus possible internal reddening within M31 itself. Cohen (1973, 1975) has shown that the correlation between reddening and the equivalent width of interstellar Na D lines has an intrinsically wide dispersion within our own Galaxy, with the ratio $E(B-V)$/EW(Na D) varying by up to an order of magnitude.

In spite of these expected complications, the correlation of Na D with $Mg_2$ in Figure 5*i* appears to be reasonable for Galactic clusters, with some evidence (e.g., NGC 7078 and NGC 6712) of contamination by interstellar lines. Unfortunately, the true slope and zero point of the relation cannot be determined from these data alone, since $E(B-V)$ is as nearly well correlated with $Mg_2$ as is Na D itself for the Galactic clusters (Fig. 5*j*). (This latter correlation stems from the well-known correlation of metallicity and position in the Galaxy.) The degree of interstellar contamination by our Galaxy in the M31 spectra is furthermore unknown and could be variable over the large angular size of M31 ($\sim 3°$). The equivalent width of interstellar lines from gas within M31 itself is also unknown.

The Na D–$Mg_2$ relation is thus badly confused both by the correlation of $Mg_2$ with $E(B-V)$ for Galactic clusters and by the probable large intrinsic variation of the ratio $E(B-V)$/EW(Na D). Very high resolution spectra might eventually help in isolating any narrow-lined interstellar components that may be present. In the meantime, however, the apparent differences among the three population groups that show up in Figure 5*i* must be set aside for lack of a unique interpretation. (Rabin 1980 also pointed out anomalous Na D–Mg ratios in both galactic and M31 globular cluster spectra but interpreted them as stellar in origin. Possible interstellar-line contamination of Na D offers an alternative explanation.)

iii) *Anomalous Indices: H$\beta$ and Higher Balmer Lines*

According to the plot of H$\beta$ against $Mg_2$ in Figure 5*k*, many M31 clusters have higher H$\beta$ than their Galactic counterparts. The difference is obvious for clusters above $Mg_2 = 0.10$ but is not so clear below this level. The vertical separation in H$\beta$ for the clusters below $Mg_2 = 0.10$ is only a 1.5 $\sigma$ effect, not sta-

tistically significant, whereas above 0.10 mag the separation is formally a 4.5 $\sigma$ effect.

Higher Balmer lines also yield additional information. Summed profiles of H$\gamma$ and H$\delta$ for four clusters in M31 and four clusters in the Galaxy are compared in Figure 6. These clusters all have $Mg_2$ in the intermediate range 0.125–0.175. Deeper H$\gamma$ and H$\delta$ lines in the M31 sum are clearly evident, consistent with the enhanced H$\beta$ strengths also measured for this group. To summarize, the M31 clusters show strong Balmer-line enhancements above the level $Mg_2 = 0.10$, but the data are not accurate enough to establish a significant enhancement below this level.

Excess Balmer-line strengths in M31 clusters were first pointed out by Spinrad and Schweizer (1972), who compared image-tube spectra of M II and M13. Rabin (1980) also discussed the effect, and his overall conclusion that H$\beta$ is stronger in the M31 clusters agrees with ours. Our study and that of Rabin (1980) do not agree well in detail, however, and our H$\beta$ measures correlate rather poorly with his for 20 clusters in common. (The agreement with other features measured by Rabin is better, as noted below.)

In addition to the Galactic–M31 difference, Figure 5*k* also shows a large discontinuity in H$\beta$ strength between Galactic globular clusters and E galaxies. The discrepancy is such that galaxies have H$\beta$ strengths roughly 50% larger than metal-rich Galactic globulars if the latter are extrapolated to $Mg_2 = 0.20$. On the other hand, no discontinuity is evident when we compare galaxies to the M31 clusters; these two samples together appear to form one unbroken continuum.

It is important to establish whether any population group shows intrinsic internal scatter in H$\beta$ strength. For galaxies, preliminary analysis has shown that the scatter in H$\beta$ is consistent with observational errors (Faber *et al.* 1984*b*). To test whether H$\beta$ differences among the clusters are real, we can check whether variations in H$\gamma$ and H$\delta$ track H$\beta$ in the same sense. Visual inspection of Figure 1 reveals pairs of clusters with similar $Mg_2$ values but different strengths in H$\gamma$ and H$\delta$ as well as H$\beta$. Such pairs include V76:V196, V99:V12, V95:V92 and M II:V64 among the M31 clusters, and NGC 6637:NGC 6624 in the Galactic group. Interestingly, no significant Balmer-line variations are apparent among the classic Galactic "second-parameter" clusters, as emphasized further in § IV*c*. Indeed, NGC 6637 is the only Galactic cluster whose Balmer lines depart significantly from the mean Galactic trend. The weak Balmer lines observed for this cluster may simply be an artifact stemming from the apparent lack of horizontal-branch stars within the measuring aperture (Hartwick and Sandage 1968).

Such an aperture problem cannot affect the M31 clusters, however, since most of their light falls within the diaphragm. There would thus appear to exist real internal scatter among Balmer lines in the M31 group, a scatter that is not present among the Galactic clusters. In view of the importance of this conclusion (§ IV*c*[iv]), it needs further verification based on more spectra with higher signal-to-noise ratio.

Some discussion of the H$\beta$ index as a Balmer-line indicator is appropriate at this point. H$\beta$ is the only Balmer line that can be reliably measured in all spectra: H$\gamma$ is often confused with night-sky Hg $\lambda$4358, and H$\delta$ is badly contaminated by metal lines in metal-rich spectra. Rabin (1980) has noted that H$\beta$ is also contaminated by metal lines, but the effect can be minimized with proper definition of the index. This is demonstrated in Figure 7, which shows the Hiltner and Williams (1946) spectrum of Arcturus convolved to our resolution, with and without H$\beta$ included. Most of the equivalent width measured by the present index is clearly coming from H$\beta$.

Faber *et al.* (1984*b*) have examined metal-line contamination of H$\beta$ more quantitatively. For the stellar K giant sample, these authors have determined $\Delta$H$\beta$ residuals relative to the mean trend of H$\beta$ with temperature and correlated these residuals with $\langle$Fe$\rangle$. A small dependence of H$\beta$ on $\langle$Fe$\rangle$ may exist, but it is not significant within the present errors of measurement [$\sigma$(H$\beta$) = 0.25 Å]. In any event, it is irrelevant to the present situation, since the M31 and Galactic clusters are compared at identical values of both $\langle$Fe$\rangle$ and $Mg_2$.

iv) *Anomalous Indices:* CN

Ironically, the situation for CN (Fig. 5*l*) is the reverse of that for H$\beta$, and it is the M31 clusters that are discrepant with respect to the E galaxies, while the Galactic clusters and E

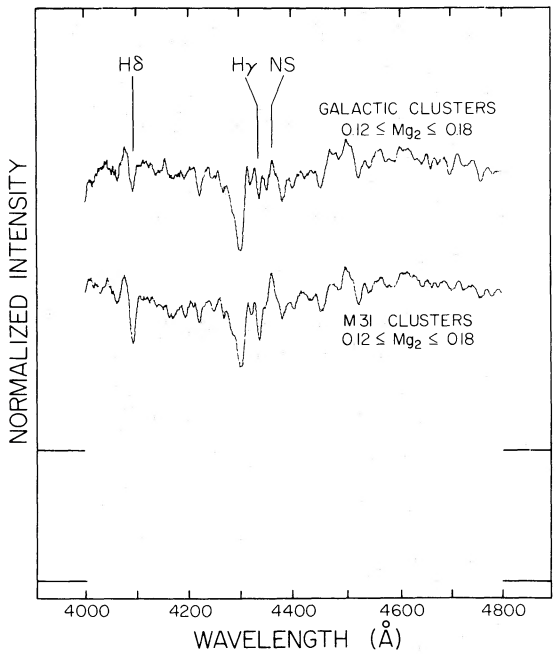


FIG. 6.—Summed spectra in the region of H$\delta$–H$\gamma$ for four M31 and four Galactic clusters in the intermediate regime $Mg_2 = 0.12$–0.18. The stronger Balmer lines show clearly in the M31 group, consistent with their larger H$\beta$ in Fig. 5*k*.

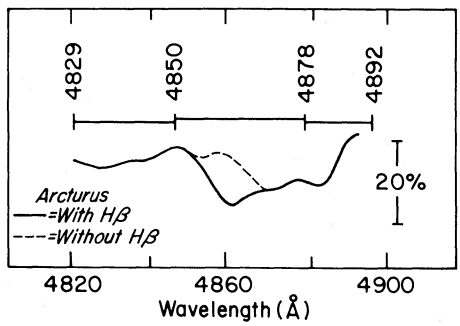


FIG. 7.—The spectrum of Arcturus from the Hiltner and Williams (1946) atlas, with and without H$\beta$ included, convolved to our spectral resolution. Continuum and central bandpasses are shown. Most of the measured equivalent width comes from H$\beta$ itself.

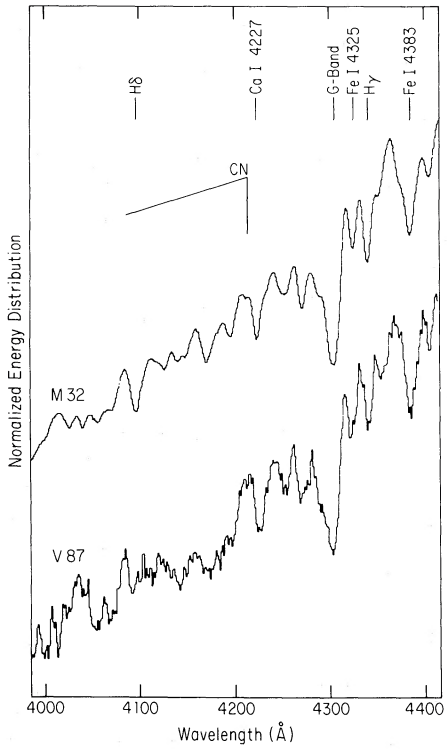


FIG. 8.—Spectra in the CN region of M32 compared with the M31 cluster V87. All other line and color indices of the two objects match closely, yet CN is markedly stronger in V87. V87 is typical of the CN enhancement exhibited by the four strong-lined M31 clusters.

galaxies follow a more or less continuous trend. The negative values of CN in Figure 5*l* are an artifact caused by the fact that the blue sideband of CN is centered squarely on H$\delta$, an unfortunate but unavoidable constraint imposed by metal-rich galaxy spectra.

For CN, it is convenient to divide the M31 clusters into three groups according to metallicity: $Mg_2 \geq 0.18$; $Mg_2$ between 0.12 and 0.18; and $Mg_2 \leq 0.12$. For the first, or metal-rich, group a large CN enhancement in M31 clusters relative to galaxies is established beyond doubt. No comparison to Galactic clusters can be made, however, since no Galactic clusters exist in this metallicity range. An example of the markedly stronger CN in the metal-rich group is shown in Figure 8, which compares the M31 cluster V87 with the elliptical galaxy M32, each of which has otherwise similar line strengths. Figure 5*l* further shows that several M31 clusters have CN strengths that rival those of the strongest-lined galactic nuclei.

A CN enhancement is not as immediately clear among the intermediate-metallicity group. The raw CN indices of M31 and Galactic clusters are nearly identical in this range, but allowance should be made for the dual effects of greater blue stellar light and higher H$\delta$ sideband contamination in the M31 clusters. An estimate of the latter is made in Figure 9, which compares the summed CN spectra of Galactic and M31 clusters in the intermediate group. The figure shows two different ways of measuring CN. The solid lines show the local continuum level and sidebands actually used here, and the dashed lines show the effect of an alternate blue sideband displaced to avoid H$\delta$. This shift of the blue sideband away from H$\delta$ increases CN by 0.03 mag in the M31 clusters relative to the Galactic clusters (see legend for Fig. 9). CN furthermore *looks* somewhat stronger in the M31 sum, judging from the bigger dip that is visible within the CN measuring interval. The above shift in sideband compensates for H$\delta$ but does not yet take into account the further problem of greater warm-star dilution of CN in the M31 clusters. In view of this additional effect, we think there is a strong possibility that CN is enhanced in the intermediate group as well as in the most metal-rich group of M31 clusters.

The situation is least clear for the metal-poor group ($Mg_2 \leq 0.12$). Summed spectra like those in Figure 9 are inconclusive. Interesting differences in the CN region between the M31 and Galactic clusters seem to be visible, but at a level that is comparable to the signal-to-noise ratio. It is obviously important to establish whether a CN enhancement extends to the metal-poor M31 clusters, but future work must employ the stronger CN 3800 Å band, as CN 4215 Å is simply too weak.

### *d) Ground-based Colors*

For completeness, Figures 10*a*–10*d* plot several broad-band colors against $Mg_2$ for globular clusters and the nucleus of M32 (measured in a 30″ aperture). Within the uncertainties of reddening (see figures), the relationships for clusters and galaxies all look similar in these diagrams. From comparison with the earlier H$\beta$–$Mg_2$ diagram, we conclude that broad-band colors are less sensitive to perturbations in the warm-star population than is H$\beta$. This insensitivity is confirmed by quantitative models below (see § IV*c*).

### *e) Other Spectroscopic Data*

Three previous investigations have compared the spectra of M31 and Galactic globular clusters. Christensen (1978) observed five clusters in M31 and five clusters in our Galaxy with the Oke multichannel scanner. Rabin (1980) observed 21

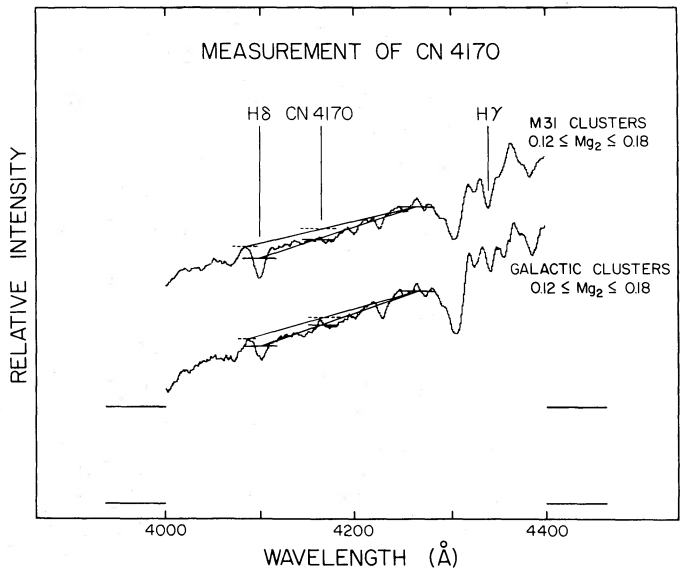


FIG. 9.—Summed spectra in the region of CN for clusters of intermediate $Mg_2$ strength ($Mg_2 = 0.12$–$0.18$): four Galactic clusters (*upper curve*), four M31 clusters (*lower curve*). Two methods of measuring CN are shown: the standard way (*solid lines*) with blue sideband on H$\delta$ and an alternate way (*dashed lines* with blue sideband shifted off H$\delta$. The two methods yield the following CN values: standard, Galactic = 0.010; alternate, Galactic = 0.033; standard, M31 = 0.011; alternate, M31 = 0.062. Elimination of H$\delta$ thus raises CN for the M31 clusters by 0.029 mag relative to the Galactic clusters. Stronger CN in the M31 clusters may be visible as the dip in the CN measuring interval.

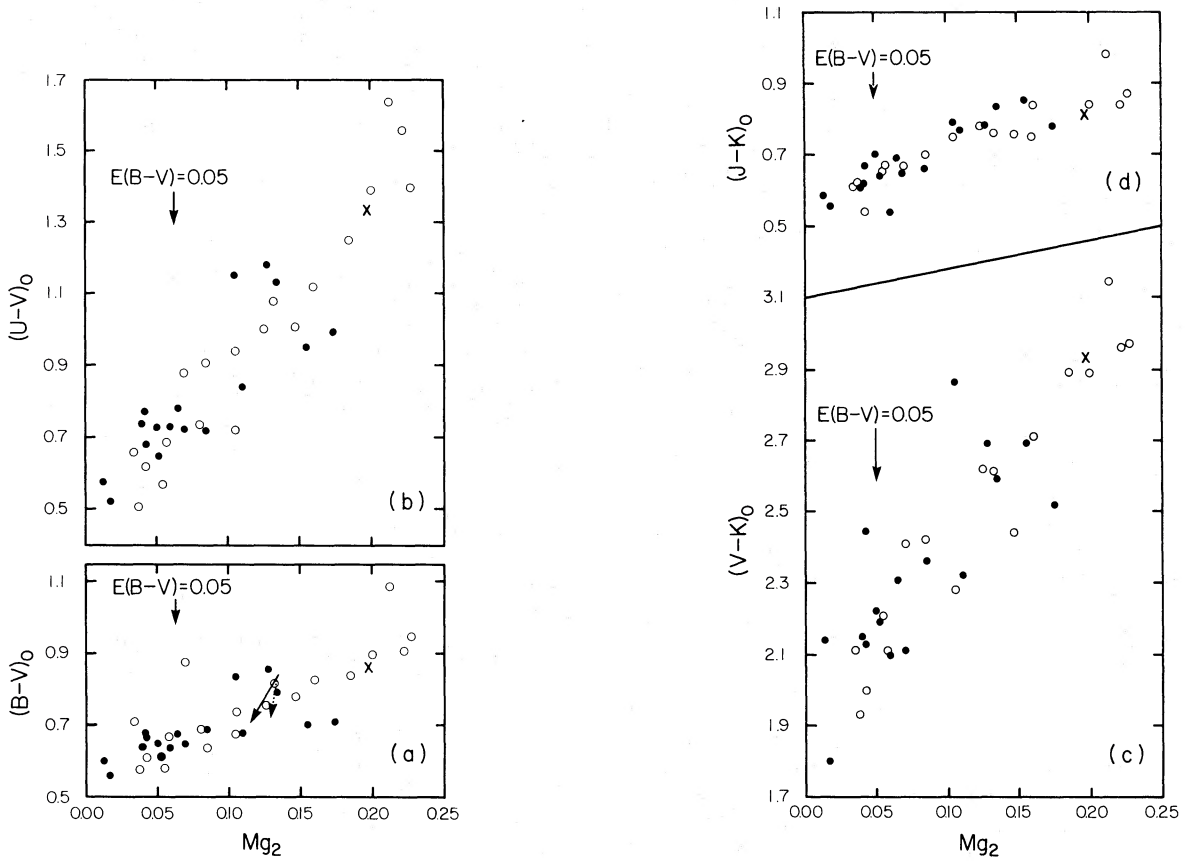


FIGS. 10*a*–10*d*.—$Mg_2$ versus four broad-band color indices for Galactic clusters (*dots*) and M31 clusters (*open circles*). The nucleus of M32 (30″ diaphragm) is plotted as a cross. A reddening uncertainty of 0.05 mag in $E(B-V)$ is indicated by the arrow. Panel *a* illustrates the effect of substituting a blue horizontal branch in 47 Tuc or M71 (*dashed arrow*; see Table 5). The effect of viewing these clusters at younger age ($5 \times 10^9$ yr) is shown by the solid arrow (see Table 5). The effect of these changes on $B-V$ is small compared with the much larger effects on H$\beta$ (in Fig. 5*k*).

M31 clusters and 13 Galactic clusters with the Palomar silicon intensified target (SIT) digital spectrograph. O'Connell (1982) combined Ca II measures by the above authors with Searle's $Q_K$ plus his own Ca II observations of Galactic globular clusters and galaxies. Using our then-unpublished $Mg_2$ measures, O'Connell (1982) constructed a Ca II–$Mg_2$ diagram similar to those of Figures 5*a*–5*l*. From this diagram, it appears that Ca II is enhanced in both Galactic and M31 clusters relative to galaxies. Thus, like H$\beta$ and CN, Ca II may be an index that reveals these three stellar populations as distinct groups.

We have also compared our $Mg_2$, CN, and H$\beta$ indices with Rabin's Mg *b*, CN 3800 Å, and H$\beta$ measures for 11 Galactic and nine M31 clusters in common, plus the nucleus of M31. Although the agreement in H$\beta$ is poor, as noted above, the Mg and CN indices for the clusters compare rather well. On the other hand, it would appear that Rabin's line strengths for the nucleus of M31 are all much too weak. This error shows up not only in comparison with our measures in Figures 5*a*–5*l* but also relative to numerous previously published values (Spinrad and Taylor 1969; O'Connell 1976; Cohen 1979). Note also that Rabin's strongest-lined object, K204, is actually a star, on the basis of its spectral-line indices as well as its stellar appearance as reported by Battistini *et al.* (1980).

### *f*) *Aperture Effects and Internal Inhomogeneities*

This section considers, then rejects, two phenomena that at first sight might seem to have some bearing on differences between M31 and Galactic clusters. The first of these is radial gradients within clusters, which conceivably could lead to an aperture effect between the two cluster groups. For example, horizontal-branch stars might be preferentially ejected from cluster centers owing to their low mass. Such hot stars might be included within the larger M31 apertures but excluded from the Galactic observations. Though qualitatively in the right sense to account for stronger H$\beta$ in the M31 clusters, quantitatively the mechanism is not attractive. As noted in § II, the mean metric aperture for the M31 clusters is only a factor of 2 larger than that for the Galactic clusters, whereas actual radial changes in horizontal-branch star density appear to involve much larger fractional changes in radius (roughly an order of magnitude larger, e.g., Alcaino and Wamstecker 1982). The color measurements of Chun and Freeman (1979) likewise indicate no change in Galactic clusters over the range in radii applicable here. Furthermore, even though core ejection of horizontal-branch stars works in the right sense for H$\beta$, it decreases CN, opposite to the CN enhancement seen in the M31 clusters.

A second potential effect stems from the presence of internal, star-to-star inhomogeneities within globular clusters. The major feature affected is CN, which shows a bimodal residual distribution in nearly every Galactic cluster studied to date with $[Fe/H] \geq -1.8$ (Smith and Norris 1982, 1983). These bimodal distributions may furthermore be related to irregularities in the horizontal-branch temperature distribution (Smith and Norris 1982) and thus also to H$\beta$.

In fact, however, we believe that integrated CN anomalies

between clusters are probably not much affected by star-to-star variations within clusters. For one thing, the Galactic clusters in our sample all show good agreement between integrated CN and all other indices, implying that mean CN must be a reasonably faithful follower of mean metal abundance despite possible internal scatter.[2] Furthermore, the sense of the Hβ–CN correlation within clusters is again opposite to that needed, since high CNO produces high-CN giants but cool, low-Hβ horizontal-branch stars (Renzini 1977).

To conclude, although Galactic globular clusters are evidently complex entities with marked internal structure, present evidence suggests no clear connection between these internal complexities and the gross, integrated differences between cluster groups that are at issue here.

### g) *Summary of the Observations*

We summarize the behavior of $Mg_2$ as compared with other line indices and colors.

*Galactic globulars versus E galaxies.*—There exists a large discontinuity in Hβ between Galactic globulars and E galaxies, Hβ being weak in globulars and strong in galaxies across the boundary between the two groups. The status of Na D is uncertain, but other indices and colors including CN define a smooth sequence.

*M31 globulars versus Galactic globulars.*—Comparison between these two groups is best carried out in three metallicity regimes. For very metal-poor clusters, there is no statistically significant enhancement in Hβ for the M31 clusters. CN may be enhanced, but the data do not allow a firm conclusion. For the intermediate group, there is a striking Balmer-line enhancement in M31 and a substantial possibility of enhanced CN as well. For the most metal-rich group, there is unambiguous enhancement of the Balmer lines in M31. Real scatter in Balmer-line strengths also seems to be present for M31 clusters over a wide range of metallicity. Such scatter seems to be generally absent among the Galactic clusters, with NGC 6637 a notable exception.

*M31 globulars versus E galaxies.*—There exists a large enhancement in CN for M31 clusters relative to E galaxies at equal $Mg_2$; in fact, some M31 clusters have CN strengths comparable to those of the strongest-lined galaxies. The status of Na D is again uncertain, but other indices and colors agree, including Hβ.

The above evidence implies that the stellar populations represented by these three data samples—Galactic globular clusters, M31 globular clusters, and E galaxies—are all intrinsically different. The next section examines basic constraints on the stellar ingredients needed to account for these differences.

## IV. ANALYSIS AND DISCUSSION

### a) *General Constraints on Stellar Ingredients*

We begin with a general overview of the types of stars required, independent of any specific model. Possibilities are restricted by the fact that most of the line indices and colors show no relative differences.

[2] Note that this conclusion is weakened somewhat by the fact that only one of our clusters, namely, NGC 6838, has actually been surveyed for CN variations. Integrated CN measures for the the remaining Smith and Norris clusters are badly needed.

#### i) *Warm Stars*

Stars needed to model the Balmer-line enhancements probably lie in the range B8–F9, but it is *a priori* unknown whether they are dwarfs or giants. Yamashita, Nariai, and Norimoto (1978) show that in this spectral range it is difficult to distinguish giants from dwarfs on the basis of Balmer lines alone. Standard metal-line luminosity criteria used for single stars in this range are useless for integrated spectra. Since gravity is a free parameter, there are a number of plausible warm stellar components that might explain the Balmer lines, including a younger main-sequence turnoff, a hot horizontal branch, blue stragglers, and a minority population of young stars (O'Connell 1980; Burstein *et al.* 1981; Gunn, Stryker, and Tinsley 1981).

Satellite ultraviolet colors are a powerful way to narrow the choices for warm stars, since the ratio of UV flux to Balmer-line strength varies enormously over the spectral range B8–F9 (Wu *et al.* 1980; O'Connell 1973, Turnrose 1976). The power of UV data is illustrated below in a comparison of the nearby elliptical M32 and the M31 cluster V64. These objects show similar Balmer-line enhancements but have very different UV fluxes and, hence, must have different warm-star populations.

#### ii) *Cool Stars*

Since CN is essentially absent in main-sequence stars, the CN enhancement of M31 globulars must originate in giant stars in the range G8–K5. The CN 4215 Å and CN 3800 Å bands are negative gravity indicators in G and K giants (Yamashita, Nariai, and Norimoto 1978; Janes 1975). Giant-branch stars are also substantial contributors to $Mg_2$ and Ca II K (Mould 1978; O'Connell 1976). Both of these latter features also depend on surface gravity, $Mg_2$ positively, and Ca II K negatively (O'Connell 1973).

Because CN and $Mg_2$ come largely from the same stars, any enhancement of CN relative to $Mg_2$ can, as far as we know, be caused in only two ways: (1) an excess abundance of nitrogen or carbon could increase CN but not $Mg_2$; (2) a decrease in the gravity of the giant branch, caused, for example, by younger age, could simultaneously increase CN and decrease $Mg_2$.

#### iii) *Implications*

The schemes proposed above will also alter other line indices besides Hβ and CN. A hotter main-sequence turnoff will dilute all metal-line indices and also lower gravity on the giant branch, thus raising CN and Ca II relative to $Mg_2$. An increase in the nitrogen abundance, if primordial, will alter the shape and location of the entire isochrone in the H-R diagram (Demarque 1979). Factors such as age and metal abundance will also effect the distribution of stars along the horizontal branch. In short, the distribution of stars in the entire H-R diagram must be considered as a whole and the strength of all line indices modeled in parallel. A thorough exploration of these effects is beyond the present capabilities of stellar libraries and theoretical models, but some aspects of the problem can be explored in a simple way. A brief discussion is presented in the following sections.

### b) *Galactic Globular Clusters versus E Galaxies: The Nearby Elliptical M32*

Among the three stellar-population groups studied here, the Galactic globular clusters are by far the best understood. Many H-R diagrams of Galactic globulars are now known, and, although there are still several unexplained phenomena, broadly speaking these diagrams are in accord with theoretical

expectations (e.g., Vanden Berg 1983). We ourselves have successfully computed a few integrated spectral indices for Galactic clusters based on their observed H-R diagrams (see § IV*c*). For the present, we assume that the Galactic globular clusters are relatively well understood, fiducial systems, against which the E galaxies and M31 clusters can be compared.

The present section treats E galaxies relative to Galactic globulars. Unfortunately, most E galaxies in the sample have $Mg_2 \geq 0.28$ mag and are thus much stronger-lined than even the most metal-rich Galactic clusters, all of which have $Mg_2 \leq 0.18$. Comparison between such different populations would be quite risky. However, there do exist a few weak-lined, low-luminosity E galaxies with $Mg_2 \sim 0.20$. These systems *can* be safely compared with the clusters, since relatively little extrapolation in line strength is involved. The nearby elliptical M32 is the best studied of these objects, having been the object of several stellar-population syntheses (Spinrad and Taylor 1969; Faber 1972; O'Connell 1980; Pritchet 1977). Complete flux measurements also exist from the far-UV (Johnson 1979; Wu *et al.* 1980) to the near-infrared (Frogel *et al.* 1978). Since all population syntheses of M32 have achieved an excellent fit with local, solar-abundance giants, the majority, cool-star population is apparently fairly well modeled, a prerequisite to understanding any minority, warm-star component. Furthermore, although the structural properties of M32 may be peculiar as a result of tidal truncation (Rood 1965; Faber 1973*b*; King and Kaiser 1973), the optical spectrum is completely typical of other small E galaxies with similar $Mg_2$. Spectrally speaking, it can therefore be regarded as a prototype small E. For all these reasons, the present discussion of E galaxies focuses entirely on the single object M32.

The sole difference between the optical data on M32 relative to those for metal-rich Galactic globulars is an enhancement in H$\beta$ of 50%. This large enhancement imposes a severe constraint on acceptable astrophysical models and, for example, immediately rules out minority metal-poor horizontal-branch stars. The presence of such stars can be modeled by adding the integrated light of a metal-poor globular cluster (H$\beta$ = 2.5 Å) to a metal-rich base population (H$\beta$ = 1.5 Å). To match a typical small E with H$\beta$ = 2.2 Å, 70% of the light would have to come from the "minority" metal-poor component, in clear violation of the overall spectral energy distribution and line strengths of small E galaxies. This conclusion is not new (cf. O'Connell 1980; Gunn, Stryker, and Tinsley 1981).

Choosing among the remaining possibilities for a warm-star population is difficult on the basis of optical data alone. However, the choice is considerably narrowed by the available UV colors $(2200 - V)$ and $(2500 - V)$ (Johnson 1979; C. C. Wu 1983, private communication). The problem is how to increase H$\beta$ significantly in M32 without at the same time making the UV colors too blue.

The stellar UV colors of Wu *et al.* (1980) plus our stellar H$\beta$ widths (see Appendix) can be used to test this constraint. We make models starting with a metal-rich base containing only cool stars later than spectral type G2. To approximate H$\beta$ and $(2200 - V)$ for this base, we use all cool stars later than G2 in O'Connell's (1980) model of M32. Various main-sequence stars are then added to the base, in amounts sufficient to increase H$\beta$ to the observed value in M32. A second set of models is also calculated to test the sensitivity of the results to the assumed H$\beta$ strengths of both the base model and M32. A fuller description is given in the legend to Figure 11.

The results show that H$\beta$ cannot be modeled by the addition of pure, early A-star light to a metal-rich base, because the resultant UV continuum will be 1.3 mag too bright. One is forced toward later F stars, whose UV colors are up to 2 mag redder but whose H$\beta$ indices are at least half as large as those of the A stars. A major contribution to the visible light of order 25% seems to be needed (see Fig. 11), which must consist mainly of quite late F stars. These stars could be either dwarfs or giants (§ IV*a*).

Evidence for late F stars in M32 has appeared consistently in earlier studies. Wu *et al.* (1980) found a strong requirement for F6–F8 stars when modeling the UV spectrum of M31, whose UV colors closely resemble those of M32. Bruzual (1981) computed evolutionary models and found a close match to the UV continuum of M32 at intermediate ages, when late F stars dominate the turnoff. O'Connell (1980) also found a fit to the entire ground-based energy distribution of M32 with a turnoff at F6–F9. O'Connell's model is a fair match to our data on small E galaxies, with a calculated H$\beta$ index of 2.0 Å.

If confirmed by future comprehensive population syntheses (which should incorporate both UV and IR light), the requirement that ~25% of the light originate in late F stars will pose a very strong astrophysical constraint. Twenty-five percent is comparable to the amount of light produced by all turnoff stars in this age range (O'Connell 1980). Blue straggler models are therefore essentially ruled out, since the number of blue stragglers would rival the number of turnoff stars. A minority component of young F stars seems equally implausible for similar reasons. The required quantity of warm star light also appears to be 50% larger than the total emitted by the horizontal branch (see Appendix), making horizontal-branch models unattractive. In view of the close match with turnoff models, O'Connell (1980) has already argued strongly that age is the culprit and the turnoff in M32 is really at late F. We have formerly been unwilling to accept this view because it seems to imply disturbingly low ages for small E galaxies, and hence by implication for E galaxies in general, but the present combination of UV colors and H$\beta$ measurements does add weight to O'Connell's interpretation.

These remarks apply only to small E galaxies like M32, since only their composition is close to solar and only their spectra are simple to model.[3] However, the problem of warm-star contamination is not confined to small E galaxies but extends to giant E galaxies as well, as is indicated not only by H$\beta$ (Fig. 5*k*) but also by numerous satellite UV observations. Gunn, Stryker, and Tinsley (1981) have studied giant E galaxies, and it is their opinion that the intermediate-temperature light in these galaxies cannot come from young turnoff stars. They instead favor choices based on very young stars, hot horizontal branches, or blue stragglers, and, in all cases, their preferred mix of light is about one-third A stars and two-thirds late- or mid-F stars. If applied to M32, these models fall short by a factor of 2 in matching its observed H$\beta$ excess, yet the match to strong-lined E galaxies could be rather better because their H$\beta$ excess is smaller (Fig. 5*k*). The important point is that the line indices, metallicity, turnoff color, and giant branches are so different in the two classes of ellipticals, that conclusions reached for one class on the basis of spectral synthesis need not necessarily apply to the other. We ourselves plan eventually to

[3] Indeed, a strict constructionist might point out that these arguments apply rigorously only to M32 itself, since no UV flux measurements yet exist for any other small E, and, without the UV flux, no constraint on warm stars can be inferred.

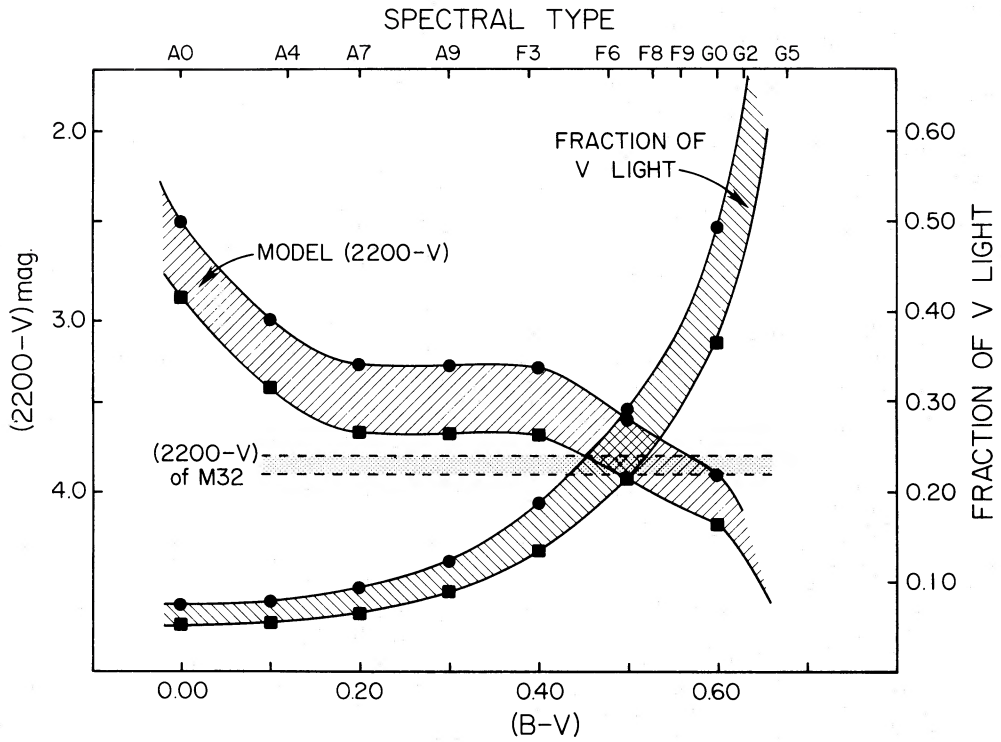


FIG. 11.—This figure summarizes the results of models to match Hβ in M32. The models start with a metal-rich base containing only cool stars later than G2 on the main sequence and giant branch. To calculate Hβ and $(2200 - V)$ for this base, we use the proportions of cool stars in O'Connell's (1980) model of M32. This yields $H\beta_{base} = 1.32$ Å and $(2200 - V)_{base} = 6.30$ mag. Different main-sequence stars are added to this base to increase Hβ to its observed value in M32. These models are represented by the solid dots. The fraction of $V$ light in the main-sequence component and the $(2200 - V)$ color are plotted for each model against the type and color of the main-sequence addition. A second series of models (*solid squares*) explores the effects of errors. This series utilizes $H\beta_{base} = 1.5$ Å and $H\beta_{M32} = 2.1$ Å, both of which reduce the hot main-sequence light required. This second series stretches the errors to reasonable limits. For discussion of models see text.

model giant ellipticals but have not yet done so because our IDS stellar library is incomplete.

### c) *Galactic Globular Clusters versus M31 Globular Clusters*

This section compares M31 and Galactic globular clusters. Although the status of CN in the M31 clusters is somewhat unclear, one is obliged at minimum to explain the strong Hβ enhancement that seems to affect basically all M31 clusters with $Mg_2$ above 0.10, as well as the CN enhancement that appears strongly above $Mg_2 = 0.18$. A CN enhancement in the intermediate range $Mg_2 = 0.12$–$0.18$ may also exist, and its consequences should be considered where appropriate.

#### i) *Anomalous Horizontal Branches and the "Second-Parameter" Effect*

One circumstance capable of producing Balmer-line enhancement is an anomalously blue horizontal branch. This mechanism should work well only at high metallicities, since the Balmer-line strengths produced by the blue horizontal branches in metal-poor Galactic clusters are already near maximum strength. This expectation is consistent, however, because the Hβ excess in M31 clusters sets in only above $Mg_2 = 0.10$, just the point where Galactic globulars are developing red horizontal branches.

Anomalous temperature variations of the horizontal branch are well known among Galactic globulars, the so-called second-parameter effect (e.g., Zinn 1980*b*). Three classic second-parameter clusters are contained in the present sample, and we were at first surprised to find no Hβ differences that parallel their horizontal-branch morphologies (see § III*c*[iii]) (Rabin 1980 noted the same absence of effect). It turns out, however, that no measurable Hβ differences are expected, since simple models show that the effects are smaller than the observational errors.

The details of these models are discussed in the Appendix, but a brief description is given here. Each model starts with a base that contains only the main-sequence, subgiant, and giant branches. The second-parameter clusters, M3, M13, and NGC 7006, as well as the comparison cluster M5, can all be represented by the same base model. Various horizontal-branch populations are added to this base, with temperature distributions as observed in the four clusters. $B-V$ and Hβ values for the base model, the individual horizontal branches, and the final models are given in Table 4.

These four horizontal branches range in integrated $B-V$ from +0.01 (M13) to +0.29 (NGC 7006). For populations as blue as these, the flux contribution of the branch at Hβ decreases monotonically with increasing blueness owing to a higher bolometric correction. As a result, the net Hβ equivalent-width contributions ($S_{H\beta}$ in Table 4) of all four branches turn out to be comparable. The end prediction is that Hβ among these four clusters should vary by only ~0.2 Å, an amount which is smaller than the errors of measurement.

In a similar calculation, Rabin (1980) has concluded to the contrary that the integrated Balmer-line difference between M13 and NGC 7006 should be large. However, Rabin did not explicitly calculate the expected Balmer-line width for NGC 7006; he extrapolated instead from the very red branch of 47 Tuc. The horizontal branch of NGC 7006 is actually quite a bit

TABLE 4

THE SECOND-PARAMETER EFFECT ON Hβ

| Model Components | $C_V$[a] | $C_B$[a] | $C_{H\beta}$[a] | $B-V$[b] | EW(Hβ)[b] (Å) | $S_{H\beta}$[c] | Base plus Horizontal Branch[d] EW(Hβ) (Å) Model | Obs. | $B-V$ Model | Obs. |
|---|---|---|---|---|---|---|---|---|---|---|
| Metal-poor "base" model: main-sequence plus giant branch[e] | 100 | 50 | 79 | 0.74 | 1.80 | 1.42 | ... | ... | ... | ... |
| Horizontal branches: | | | | | | | | | | |
| M13 | 11 | 11 | 11 | 0.01 | 8.14 | 85 | 2.55 | 2.25 | 0.65 | 0.67 |
| M3 | 19 | 15 | 18 | 0.25 | 5.62 | 99 | 2.50 | 2.44 | 0.65 | 0.68 |
| N7006 | 21 | 16 | 19 | 0.29 | 4.99 | 93 | 2.41 | 2.38 | 0.65 | 0.64 |
| M5 | 17 | 15 | 16 | 0.14 | 6.30 | 102 | 2.57 | 2.29 | 0.63 | 0.68 |

[a] Relative contributions in arbitrary units at $V$, $B$, and Hβ, normalized to 100 for $C_V$ of base model.
[b] $B-V$ and Hβ for each model component.
[c] $C_{H\beta} \times$ EW(Hβ).
[d] Sum of "base" plus horizontal branch. Observed values refer to the four clusters.
[e] See Appendix.

bluer than that of 47 Tuc, owing to a substantial RR Lyrae population that contributes nearly half the flux at Hβ (see Appendix).

The above models suggest that horizontal-branch effects on Hβ should be small for Galactic metal-poor clusters. On the other hand, both Rabin and we agree that a large Balmer-line enhancement is expected when a blue horizontal branch is substituted for the very red horizontal branches that exist in metal-rich Galactic clusters. The magnitude of this enhancement can be estimated quantitatively by taking a cluster like 47 Tuc or M71 as a starting point (both have stubby, red branches) and computing what happens when the horizontal branch is changed to look like that of M5, which is such as to yield maximum Hβ strength (see Table 4). The details of this calculation appear in the Appendix, and the results are shown in Table 5 and Figure 5*k* (*dashed arrow*). Evidently a temperature shift as drastic as this appears able to match the Hβ excess of the intermediate- and metal-rich M31 clusters rather well. In contrast, the effect on $B-V$ (Fig. 10*a*, *dashed arrow*) is virtually undetectable, consistent with the observed narrow color loci.

An additional check is provided by satellite UV observations. *International Ultraviolet Explorer* (*IUE*) observations exist for just one M31 globular cluster, V64 (Cacciari *et al.* 1982), which is luckily included in the present sample. V64 is a moderately strong-lined cluster comparable to 47 Tuc or M71. Its Hβ seems a little weak for an M31 cluster (see Fig. 5*k*), but there is only one observation, and it is within 1 $\sigma$ of the mean trend. In contrast to the visual spectrum, the satellite UV flux from V64 is very blue, ranking it with the bluest Galactic clusters with extremely hot horizontal branches (the EB class of van Albada de Boer, and Dickens 1981). Cacciari *et al.* (1982) therefore suggest that V64 is a moderately strong-lined cluster with an anomalously hot horizontal branch. Consistent with this suggestion, one can fit both the general UV continuum level and Hβ with an extremely hot horizontal branch having a rather narrow temperature distribution centered on $B-V = -0.15$ and the standard number of horizontal-branch stars.[4]

Even though hot horizontal branches can explain Hβ, there is no obvious link in such a picture to enhanced CN. As we

[4] Note that V64 and M32 have nearly identical Hβ widths. The radically different hot-star populations inferred in these two objects (B stars in V64, late F stars in M32) are a consequence of their very different far-UV colors. This fact underscores the great importance of satellite UV data in accurate hot-star population syntheses.

TABLE 5

MODELS FOR GLOBULAR CLUSTERS

| Model Components | $C_V$ | $C_B$ | $B-V$ | EW(Hβ) (Å) | $Mg_2$ (mag) | CN (mag) | Final Model $B-V$ | EW(Hβ) (Å | $Mg_2$ (mag) | CN (mag) |
|---|---|---|---|---|---|---|---|---|---|---|
| *a*) Metal-rich[a] Base plus Red and Blue Horizontal Branches | | | | | | | | | | |
| Base model: metal-rich[a] main sequence plus giant branch | 100 | 44 | 0.88 | 1.41 | 0.15 | 0.02 | ... | ... | ... | ... |
| Horizontal branches: | | | | | | | | | | |
| Red: M71 | 19 | 11 | 0.61 | 1.96 | 0.06 | −0.06 | 0.83 | 1.51 | 0.135 | 0.003 |
| Blue: M5 | 17 | 15 | 0.14 | 6.30 | 0.02 | −0.18 | 0.74 | 2.31 | 0.129 | −0.042 |
| *b*) Young Model | | | | | | | | | | |
| Metal-rich:[a] $5 \times 10^9$ years old | ... | ... | ... | ... | ... | ... | 0.72 | 2.41 | 0.119: | ... |

[a] Same metallicity as 47 Tuc and M71. See Appendix.

have seen, this certainly exists among the most metal-rich M31 clusters and may exist among the intermediate group as well. The lack of explanation for CN is a serious deficiency of horizontal-branch models.

In conclusion, it could be misleading to identify too closely the extreme swings in horizontal-branch temperature required in M31 globulars with the second-parameter effect among Galactic globulars. The classic second-parameter clusters are found only in a restricted metallicity range ([Fe/H] = −1.7 to −1.2; Zinn 1980*b*), whereas Balmer-line enhancements are seen over a very wide metallicity range in M31. Therefore, even if large horizontal-branch differences are present in M31, their cause may well differ from that of the Galactic second-parameter effect. Actually, a plausible theory for hotter horizontal branches in M31 is not easy to find, since most of the obvious mechanisms, e.g., higher $Z_{CNO}$ or younger age, should produce cooler, not hotter, horizontal branches (but see also § IV*c*[iii]).

ii) *Blue Stragglers*

The idea of excess blue stragglers in M31 globulars is a slippery hypothesis that is difficult to test. The hypothesis is flexible because the temperature distribution of blue stragglers along the main sequence is unconstrained by theory. Galactic clusters that contain blue stragglers show considerable variation in this distribution and provide only vague guidelines as to what it should be in other systems. The crucial parameter is how many hot stars with high H$\beta$ there are relative to cooler stars near turnoff. The more hot stars there are, the fewer blue stragglers are required to match H$\beta$.

We have surveyed Galactic-cluster H-R diagrams containing blue stragglers (M67, M3, NGC 7789, NGC 188) and computed a few models based on the temperature distributions of stragglers so determined. A useful ratio, $S$, is the number of blue stragglers relative to the number of main-sequence and turnoff stars within $\pm 1$ mag of the turnoff point. For these four clusters, the mean value of this ratio is 0.12 (0.09 minimum, 0.16 maximum). In all four clusters, there are substantial numbers of hot blue stragglers, and the H$\beta$ enhancements in M31 are consequently well matched with modest values of $S$ between 0.05 and 0.13.

These models are successful because Galactic blue stragglers contain large numbers of A stars. Such A stars would of course produce their usual bright signature in the UV. Were future UV observations of M31 clusters to rule out such stars, the blue-straggler population would have to be truncated at mid-F types. Their absolute numbers would then have to grow, partly because each blue straggler is in the mean fainter and partly because H$\beta$ for each star is lower. The net result is that $S$ would have to increase substantially, by at least a factor of 3 or 4. Since values of $S$ as large as 0.5 are astrophysically unreasonable, the blue-straggler hypothesis would then be effectively ruled out.

At the other extreme, discovery of many clusters with UV colors as blue as V64 would also constitute a severe blow to the blue-straggler idea. As noted above, the extremely blue UV color of V64 requires quite hot stars with $B-V \sim -0.15$. Such a color is produced naturally by a very hot horizontal branch but is quite unlike the typical color of Galactic blue stragglers, which are much cooler. Once again, it is clear that accurate UV fluxes are a key factor in testing various alternatives.

Finally, there is again the problem that blue stragglers have no obvious connection with enhanced CN. As above, it would be necessary to posit some causal relationship between CN and the production of blue stragglers.

iii) *Elemental Abundance Anomalies*

In contrast to preceding models, most theories based on abundances are aimed at explaining CN rather than H$\beta$. The most plausible idea is that nitrogen is somehow enhanced on the giant branch. For a ballpark estimate of the required enhancement in the absence of change in any other color or index, consider the following comparison: the cluster V87 in M31 has a CN index that is 0.1 mag stronger than that of M32 yet has nearly identical $Mg_2$, H$\beta$, $\langle$Fe$\rangle$, and continuum colors. Stellar synthesis models of M32 (O'Connell 1980) indicate that CN-strong giant stars contribute only 30% of the continuum flux at 4150 Å. The enhancement in integrated CN thus implies a minimum increase of 0.3 mag in the CN values of individual giant stars. Since the metallicity of M32 seems to be near solar, its giants probably have CN in the range 0.25–0.35 (Faber *et al.* 1984*a*). CN values of giants in V87 would then have to be in the range 0.55–0.65 mag, which is considerably greater than the maximum value of 0.5 mag yet seen in any solar-neighborhood K giant. These inferred values of CN are also very much larger than the measured values of 0.20–0.35 mag for normal giant stars in metal-rich Galactic clusters (Smith and Norris 1982, 1983) and are large even when compared with the values of $\sim$0.4 mag in the exceptional, strong-CN stars of $\omega$ Cen (e.g., ROA 253; Bessel and Norris 1976). Whether caused by mixing or by primordial nitrogen overabundance, CN enhancements of such striking magnitude in stars of otherwise solar composition are difficult to understand.

It therefore seems unlikely that CN by itself is enhanced. More probably, the anomalous location of the metal-rich M31 clusters in Figure 5*l* is due to some combination of *increased* CN and *decreased* $Mg_2$. This idea is carried further in the discussion of young stars in § IV*c*(iv) below.

Differences in helium content might also have detectable effects on the integrated spectrum, principally through changes in the temperature distribution of the horizontal branch. From Demarque (1979), we estimate that an increase of $\sim$0.05 in $Y$ would be required to change the red horizontal branch of a cluster like 47 Tuc into one that is moderately blue. If the present cluster sample is typical, essentially all metal-rich and intermediate M31 clusters would have to have enhanced helium, an ad hoc assumption. Moreover, increased helium by itself cannot explain enhanced CN. Although it therefore seems implausible that helium could be the sole cause of the spectral differences of the M31 clusters, helium could conceivably play a significant role if coupled with changes in age and/or the abundance of other elements.

iv) *Younger Ages*

In a final attempt to account for the M31 globular clusters we have tried to explore very roughly the effects of younger age. We start with a cluster of the age and metallicity of M71 and ask what it would have looked like at an age of only $5 \times 10^9$ years. The models are too crude to warrant detailed description here, but basically we started with the metal-rich M71 base model of the Appendix and Table 5 and perturbed its turnoff temperature and giant branch to reflect younger age using differential shifts from the Ciardullo and Demarque (1977) tracks. The effect of temperature changes on spectral features was estimated from the stellar library. A few estimated indices are given in Table 5, and the locations of the model are shown in Figures 5*k* and 10*a* (*tips of solid arrows*). H$\beta$ and

$B-V$ are reliably estimated in this model, but the calculation of $Mg_2$ does not yet take into account the change in both temperature and gravity of the giant branch. It is also not possible yet to estimate CN.

Nonetheless, the large increase in H$\beta$ that can be obtained with this mechanism is rather encouraging. Our guess at the qualitative changes in other gravity-sensitive indices was outlined in § IV*a*. The lower gravity of the giant branch will strengthen CN and Ca II but weaken $Mg_2$. Younger age is thus a promising way to explain the necessary excess in CN relative to $Mg_2$ and other line indices deduced in § IV*c*(iii) above.

Three additional pieces of evidence seem to favor younger ages. Although the M31 clusters in the sample are brighter as a group than the Galactic clusters, the difference is considerably larger for those with Balmer-line enhancements (cf. Tables 2 and 3). Perhaps these clusters are more luminous because they are younger. The most metal-rich M31 clusters also have line strengths that are considerably higher than any known Galactic globulars. These could conceivably be metal-rich members of the M31 disk population, rather like NGC 2158 in our own Galaxy. Finally, there is evidence for intrinsic Balmer-line scatter among the M31 clusters, which might be explained by clusters having a range of ages.

Viewed another way, the age hypothesis might be equated with a magnitude-selection effect, stemming from the fact that we have in general observed only the brightest M31 clusters. At very low metallicities, all clusters in M31 could be old and hence true globulars. Observing only the brightest of these clusters would not introduce any age bias. At higher metallicities, there might be a range of ages and a plausible inverse correlation between age and brightness. The metal-rich M31 sample might thus have picked out preferentially young clusters from among the total. This discussion highlights the need for deeper surveys of M31 to verify whether the present sample is in fact representative of the cluster system as a whole.

Ultraviolet fluxes will ultimately provide the best test of ages for the M31 clusters. To match H$\beta$, young, solar-composition clusters must have a turnoff at ~F5, cool enough that the far-UV colors should be quite red. Discovery of many more extremely blue clusters like V64 among the metal-rich group would thus rule out younger age as the sole source of the M31 line-strength anomalies.

### *d) Metal-rich M31 Clusters versus M32: A Puzzle*

Of the mechanisms discussed above for the metal-rich M31 clusters, only one—younger age—appears able even in principle to account simultaneously for both H$\beta$ and CN. Simple models seem to require an age of roughly $5 \times 10^9$ years to match these clusters. On the other hand, O'Connell (1980) has deduced a very similar age for M32 based on its Balmer-line strength and continuum colors. This similarity in estimated age is not surprising, since the Balmer lines of M32 and the metal-rich M31 clusters are essentially identical.

In this context, it is noteworthy that CN in M32 and the M31 clusters is *not* in fact the same. Thus, although M32 and the clusters may all in fact be young, it is probable that at least one more fundamental difference between the two must remain. Alternatively, the M31 clusters might be even younger than M32, but, if so, we would require that CN be a steep function of age in this age-metallicity regime. Clearly, a consistent picture of M32 vis-à-vis the M31 clusters has not yet emerged.

## V. SUMMARY AND CONCLUSIONS

We originally planned to use the globular clusters in the Galaxy and in M31 as basic ingredients in stellar population models for elliptical galaxies. Unfortunately, the situation turned out to be more complicated than we had hoped, and we find that these three population groups are all somehow fundamentally different from one another. For elliptical galaxies, the main difference is a sizable enhancement in H$\beta$ relative to Galactic globulars. In the small elliptical M32, accounting for its H$\beta$ excess without making the UV flux too blue requires late F stars as opposed to hotter types. The number of these stars is commensurate with their actually being at the true main-sequence turnoff. In view of the fact that all E galaxies from small to large exhibit an unbroken continuum in spectra, it is both surprising and disturbing that M32 is so at variance with the conclusions of Gunn, Stryker, and Tinsley (1981) on warm stars in giant ellipticals. This is a matter which clearly must be looked into more deeply.

The differences between M31 and Galactic clusters seem to increase with line strength. For H$\beta$, a statistically significant enhancement emerges near $Mg_2 = 0.10$ mag and grows above this level. For CN, evidence of enhancement relative to the Galactic clusters becomes suggestive in the interval $Mg_2 =$ 0.12–0.18 mag. If the M31 clusters are further compared to elliptical galaxies, a striking enhancement in CN sets in at $Mg_2 = 0.20$ mag and grows above this level. In addition to these global differences, there also appears to be significant intrinsic scatter in Balmer lines among the M31 sample. (No such scatter is evident at present among the E galaxies, or, with one exception [NGC 6637], among the Galactic clusters.)

Several mechanisms might in principle account for the general Balmer-line excess of the M31 clusters, including anomalously blue horizontal branches, blue stragglers, or younger age. The extremely blue *IUE* flux of the intermediate cluster V64 seems to imply a large group of fairly hot stars with $B-V \sim -0.15$. Of the above options, a hot horizontal branch would be most consistent with such a population.

Enhanced CN can originate only on the giant branch. As far as we know, it can be enhanced relative to $Mg_2$ in only one of two ways: increased nitrogen and/or carbon, or a large decrease in the gravity of the giant branch. The former mechanism appears unlikely, because it would require CN band strengths that greatly exceed those of any solar-neighborhood K giants. Of the several mechanisms that might cause lower gravity, younger age looks most promising, since it alone might also explain enhanced H$\beta$ in the same clusters.

Following this evidence, if one now concludes that M32 and the metal-rich M31 clusters are all relatively young, a further puzzle emerges since CN is very different in the two groups. No convincing explanation for this additional difference is as yet apparent.

Far-UV satellite fluxes plus accurate Balmer-line strengths are the best way to narrow down choices for warm stars. Direct measurements of horizontal-branch morphology in M31 and M32 using Space Telescope will also provide key input. Better observations of the gravity indicator Ca II K are also useful, as well as the strong CN band at 3800 Å. Finally, there is a strong need for accurate data on a larger and fainter sample of clusters in M31. This is essential to test whether the present sample of 19 objects is seriously biased by the inclusion of only the brightest M31 clusters.

In conclusion, the main result of this paper is that old stellar

populations which up to now have looked superficially similar can show surprising variations when the observational material is refined. Still better data may uncover yet more differences and, we hope, more clues to the origin and evolution of both elliptical galaxies and globular clusters.

We would like to thank past and present directors of Lick Observatory for continued generous amounts of observing time on the Shane 3 m telescope. Special thanks go also to Drs. Joseph Wampler and Lloyd Robinson and the staff of the Lick Observatory technical shops and mountain crew for their development and maintenance of the image-dissector scanner and its associated software. The stability and reliability of this instrument over an eleven-year period is a remarkable achievement and is responsible for the homogeneity of the present data base. Further thanks go to Robert Kibrick of Lick Observatory for his special programming of the Shane telescope to allow raster scanning of the Galactic globulars. We thank Dr. Robert W. O'Connell and especially Dr. Albert Whitford for many valuable discussions on old stellar populations over the past decade. Most of this work was supported by NSF grants AST 76-08258 and AST 82-11551 and the UC Santa Cruz Faculty Research Committee.

## APPENDIX

## SEMIEMPIRICAL STELLAR POPULATION MODELS

### I. METAL-RICH BASE MODEL FOR GLOBULAR CLUSTERS

This model is used in § IV*c*(i) to study the effect of horizontal-branch variations on H$\beta$. It contains the main-sequence and giant branches of the two clusters M71 and 47 Tuc, here assumed to be identical and treated interchangeably. The basic data for the model include IDS spectra of 110 solar-neighborhood K giants of a wide range of abundance and temperature (Faber *et al.* 1984*a*), two K giants from M71 itself, and a wide variety of main-sequence stars from the solar neighborhood. The bolometric luminosity function used is an average of the empirically measured functions for 47 Tuc (Hesser and Hartwick 1977) and M92 (Hartwick 1970). These agree well with one another and also with the theoretical function of Ciardullo and Demarque (1977; $Y = 0.2$, $Z = 0.01$, $t = 13 \times 10^9$ yr). Bolometric corrections as a function of $B-V$ were taken from Frogel, Persson, and Cohen (1980). Line strengths were assigned to each point on the model isochrone on the basis of observed $(B-V)_0$ in 47 Tuc by interpolation in the stellar library [$E(B-V) = 0.04$ mag and [Fe/H] $= -0.5$ were assumed for 47 Tuc]. Rough corrections amounting to 6% of the $V$ light correct for the missing lower main sequence.

### II. BASE MODEL FOR M13, M3, NGC 7006, AND M

These clusters have such low metallicity ([Fe/H] $\sim -1.1$ to $-1.5$) that a base model could not be constructed as outlined above owing to the present lack of low-metallicity dwarfs in the stellar library. We therefore attempted to estimate just $B-V$ and H$\beta$ for a base model in two different ways. One way involved a crude correction to the $B-V$ and H$\beta$ of the previous model based on the blueward shift of the whole H-R diagram locus relative to M71 and 47 Tuc. The second utilized the integrated values of $B-V$ and H$\beta$ for NGC 7006, minus the known horizontal-branch component (see below). The two methods agreed rather well, and the resultant mean values for H$\beta$ and $B-V$ are given as the base population in Table 4.

TABLE 6

EW(H$\beta$) AS A FUNCTION OF $B-V$ FOR HORIZONTAL BRANCH STARS

| $B-V$ | EW(H$\beta$) (Å) |
|---|---|
| −0.1 | 7.5 |
| 0.0 | 8.6 |
| 0.1 | 8.5 |
| 0.2 | 7.6 |
| 0.3 | 6.2 |
| 0.4 | 4.9 |
| 0.5 | 3.7 |
| 0.6 | 2.9 |

### III. HORIZONTAL-BRANCH MODELS FOR M13, M3, NGC 7006, M5, AND M71

The basic distributions of horizontal-branch stars in $B-V$ color were taken from color-magnitude diagrams published by Arp (1955, 1962; M13, M3, M5), Sandage and Wildey (1967; NGC 7006), and Hesser and Hartwick (1977; M71). The relative numbers of RR Lyrae stars were estimated from the same physical areas of the cluster used to obtain the other horizontal-branch stars. The calculated RR Lyrae star contributions to the total horizontal-branch continuum at H$\beta$ ($C_{H\beta}$ in Table 4) are 40% (M5), 50% (M3), 29% (NGC 7006), and 2% (M13). The calculated contributions of RR Lyrae stars to the equivalent width of H$\beta$ are 35% (M5), 48% (M3), 43% (NGC 7006), and 1% (M13). Note the importance of the RR Lyrae contribution to the equivalent width for NGC 7006.

H$\beta$ and other line-strength values were assigned by interpolation using the H$\beta$–$(B-V)_0$ relationship for the stellar library (Table 6), which contains 25 horizontal-branch stars from five globular clusters and the field. The actual number of horizontal-branch stars was determined using Renzini's (1977) ratio of horizontal-branch to giant-branch stars (1.6) obtained from star counts in several clusters. Renzini's ratio is also close to the mean of M92 and 47 Tuc based on the luminosity functions used by us. This value for the number of horizontal-branch stars, assumed to be the same in all models, then leads to the fractional light contributions of the horizontal branch listed in Tables 4 and 5.

## REFERENCES

Aaronson, M., Cohen, J. G., Mould, J., and Malkan, M. 1978, *Ap. J.*, **223**, 824.
Aaronson, M., and Malkan, M. 1983, in preparation.
Alcaino, G., and Wamstecker, W. 1982, *Astr. Ap. Suppl.*, **50**, 141.
Arp, H. 1955, *A.J.*, **60**, 317.
———. 1962, *Ap. J.*, **135**, 311.
Baade, W. 1944, *Ap. J.*, **100**, 137.
Battistini, P., Bonoli, F., Braccesi, A., Fusi Pecci, F., Malagnini, L., and Marano, B. 1980, *Astr. Ap. Suppl.*, **42**, 357.
Baum, W. A. 1955, *Pub. A.S.P.*, **67**, 328.
Bessel, M. S., and Norris, J. 1976, *Ap. J.*, **208**, 369.

Bruzual, G. 1981, Ph.D. thesis, University of California, Berkeley.
Burstein, D. 1979, *Ap. J.*, **232**, 74.
Burstein, D., *et al.* 1985, in preparation.
Burstein, D., Faber, S. M., Gaskell, C. M., and Krumm, N. 1981, in *IAU Colloquium 68, Astrophysical Parameters for Globular Clusters*, ed. A. G. D. Philip and D. S. Hayes (Schenectady: Dudley Observatory), p. 441.
Burstein, D., and Heiles, C. 1978, *Ap. J.*, **225**, 40.
———. 1982, *A.J.*, **87**, 1165.
Burstein, D., and McDonald, L. H. 1975, *A.J.*, **80**, 17.
Cacciari, C., Cassatella, A., Bianchi, L., Fusi Pecci, F., and Kron, R. G. 1982, *Ap. J.*, **261**, 77.
Christensen, C. G. 1978, *A.J.*, **83**, 244.
Chun, M. S., and Freeman, K. C. 1979, *Ap. J.*, **227**, 93.
Ciardullo, R. B., and Demarque, P. 1977, *Yale Trans.*, Vols. **33–35** (New Haven: Yale University Press).
Cohen, J. G. 1973, *Ap. J.*, **186**, 149.
———. 1975, *Ap. J.*, **197**, 117.
———. 1979, *Ap. J.*, **228**, 405.
Demarque, R. 1979, in *IAU Symposium 85, Star Clusters*, ed. J. E. Hesser (Boston: Reidel), p. 281.
Faber, S. M. 1972, *Astr. Ap.*, **20**, 361.
———. 1973*a*, *Ap. J.*, **179**, 731.
———. 1973*b*, *Ap. J.*, **179**, 423.
———. 1977, in *The Evolution of Galaxies and Stellar Populations*, ed. B. M. Tinsley and R. B. Larson (New Haven: Yale University Press), p. 157.
Faber, S. M., Burstein, D., Dalle Ore, C., and Gaskell, C. M. 1984*b*, in preparation.
Faber, S. M., Friel, E., Burstein, D., and Gaskell, C. M. 1984*a*, *Ap. J., Suppl.*, in press.
Frogel, J. A., Persson, S. E., Aaronson, M., and Matthews, K. 1978, *Ap. J.*, **220**, 75.
Frogel, J. A., Persson, S. E., and Cohen, J. G. 1980, *Ap. J.*, **240**, 785.
Gunn, J. E., Stryker, L. L., and Tinsley, B. M. 1981, *Ap. J.*, **249**, 48.
Harris, W. E., and Racine, R. 1979, *Ann. Rev. Astr. Ap.*, **17**, 241.
Hartwick, F. D. A. 1970, *Ap. J.*, **161**, 845.
Hartwick, F. D. A., and Sandage, A. 1968, *Ap. J.*, **153**, 715.
Hesser, J. E., and Hartwick, F. D. A. 1977, *Ap. J. Suppl.*, **33**, 361.
Hiltner, W. A., and Williams, R. C. 1946, *A Photometric Atlas of Stellar Spectra* (Ann Arbor: University of Michigan Press).
Janes, K. A. 1975, *Ap. J. Suppl.*, **29**, 161.
Johnson, H. M. 1979, *Ap. J.* (*Letters*), **230**, L137.
King, I. R. 1971, *Pub. A.S.P.*, **83**, 377.
King, I. R., and Kaiser, J. 1973, *Ap. J.*, **181**, 27.
Kraft, R. P. 1979, *Ann. Rev. Astr. Ap.*, **17**, 309.
Liller, M. H., and Liller, W. 1976, *Ap. J.* (*Letters*), **207**, L109.
Mould, J. 1978, *Ap. J.*, **220**, 434.
O'Connell, R. W. 1973, *A.J.*, **78**, 1074.
———. 1976, *Ap. J.*, **206**, 370.
———. 1980, *Ap. J.*, **236**, 430.
———. 1982, *Highlights Astr.*, in press.
Peterson, R. C., 1981, in *IAU Colloquium 68, Astrophysical Parameters for Globular Clusters*, ed. A. G. D. Philip and D. S. Hayes (Schenectady: Dudley Observatory), p. 121.
Pilachowski, C. A., Sneden, C., and Wallerstein, G. 1983, *Ap. J. Suppl.*, **52**, 241 (PSW).
Pritchet, C. 1977, *Ap. J. Suppl.*, **35**, 397.
Rabin, D. M. 1980, Ph.D. thesis, California Institute of Technology.
Renzini, A. 1977, in *Advanced Stages in Stellar Evolution*, ed. P. Douvier (Saas-Fee: Geneva Observatory), p. 151.
Robinson, L., and Wampler, E. J. 1972, *Pub. A.S.P.*, **84**, 161.
Rood, H. J. 1965, *A.J.*, **70**, 689(A).
Sandage, A. R., and Wildey, R. 1967, *Ap. J.*, **150**, 469.
Searle, L., Wilkinson, A., and Bagnuolo, W. G. 1980, *Ap. J.*, **239**, 803.
Searle, L., and Zinn, R. 1978, *Ap. J.*, **225**, 357.
Smith, G. H., and Norris, J. 1982, *Ap. J.*, **254**, 149.
———. 1983, *Ap. J.*, **264**, 215.
Smith, H. A., and Perkins, G. J. 1982, *Ap. J.*, **261**, 576.
Spinrad, H., and Schweizer, F. 1972, *Ap. J.*, **171**, 403.
Spinrad, H., and Taylor, B. J. 1969, *Ap. J.*, **157**, 1279.
Turnrose, B. E. 1976, *Ap. J.*, **210**, 33.
van Albada, T. S., de Boer, K. S., and Dickens, R. J. 1981, *M.N.R.A.S.*, **195**, 391.
Vanden Berg, D. 1983, *Ap. J. Suppl.*, **51**, 29.
van den Bergh, S. 1969, *Ap. J. Suppl.*, **19**, 145.
Wu, C. C., Faber, S. M., Gallagher, J. S., Peck, M., and Tinsley, B. M. 1980, *Ap. J.*, **237**, 290.
Yamashita, Y., Nariai, K., and Norimoto, Y. 1978, *An Atlas of Representative Stellar Spectra* (New York: Wiley).
Zinn, R. 1980*a*, *Ap. J. Suppl.*, **42**, 19.
———. 1980*b*, *Ap. J.*, **241**, 602.
———. 1984, preprint.

D. BURSTEIN: Physics Department, Arizona State University, Tempe, AZ 85281

S. M. FABER: Lick Observatory, University of California, Santa Cruz, CA 95064

C. M. GASKELL: Department of Astronomy, University of Texas, RLM 15.212, Austin, TX 78712

N. KRUMM: Physics Department, University of Cincinnati, Cincinnati, OH 45221